بسم الله الرحمن الرحيم

Sudan University of Science and Technology

College of Graduate Studies

Estimation of Effective Dose for Abdominal Organs during Computed tomography

تقدير الجرعة الفعالة للأعضاء البطنية أثناء التصوير المقطعي

Submitted in partial fulfillment for the requirements

Of M Sc. degree in Medical Physics

By:

TAYFOUR HASSAN SAEED BAKIET

Supervisor

Dr. Hussein. Ahmed. Hassan

الآيـة

قال الله تعالى : ﴿ هُوَ الَّذِي بَعَثَ فِي الْأُمِّيِّينَ رَسُولًا مِنْهُمْ يَتْلُو عَلَيْهِمْ آيَاتِهِ وَيُزَكِّيهِمْ وَيُعَلِّمُهُمُ الْكِتَابَ وَالْحِكْمَةَ وَإِنْ كَانُوا مِنْ قَبْلُ لَفِي ضَلَالٍ مُبِينٍ ﴾

سورة الجمعة (2)

Dedication

I dedicate this work to my mother, may God have mercy on her, my father, my sons and daughters, my wife, all the brothers and sisters who stand by me and the doctors who supported me in my educational career

Acknowledgements

I would like to thank all the people who contributed in some way to the work described in this research

Foremost, I would like to express my sincere gratitude to my Supervisor Dr. Hussein. A. Hassan for the continuous support of my research, for his patience, motivation, enthusiasm, and immense knowledge. His guidance helped me during all the time of research

I especially thank Mrs. Kawther and Dr. Ahmed Abukonna for Dean of Faculty of Radiology for their support during my studies

Also, my deep thanks to my friend. Mr. Mustafa Awad who was supporting and .help me when I needed him

I would like to thank my classmate Mr. Abubaker Alsaid and Mr. Amjad for help and support me when I needed them

I am extremely grateful to my parents for their love. And also I am very much thankful to my wife Rawah and my daughters Fatima and Zainab for their love, my sons Mohammed and Ahmed

Abstract

The aim of this study to estimate the radiation dose received by the patients during abdomen CT examinations. A total of 60 adult patients undergoing abdominal CT scanning exams were estimated using $CTDI_{vol}$, dose length product (DLP) and effective dose (E) and evaluate effective dose and organs dose by using CT expo version 2.5 software.

Also this study revealed that the mean effective dose for abdomen in hospital (A), hospital (B) and hospital (C) was (7.6)mSv, (5.3) mSv and (6.3) mAs respectively. The mean of DLP for in hospital (A), hospital (B), and hospital (C) was (450) mGy*cm, (410.95) mGy*cm and (380) mGy*cm respectively. The mean $CTDI_{vol}$ for abdomen in hospital (A), hospital (B) and hospital (C) was (9.9) mGy, (8.8) mGy and (7.3) mGy respectively

The result of this study revealed that the mean equivalent dose for abdomen organs, stomach was (12.23) mSv, spleen was (11.99) mSv, pancreas was (9.8) mSv and adrenal gland was (9.158) mSv.

And the organ doses were estimated using measurements of CT dose indexes (CTDI), exposure-related parameters, and the ImPACT spreadsheet based on NRPB conversion factors. Light variation of organ doses among three hospitals was observed for similar CT examinations. These variations largely originated from different CT scanning protocols used in different three hospitals. The organ doses in this study

المستخلص

تهدف هذه الدراسة إلى تقدير جرعة الإشعاع التي تلقاها المرضى خلال فحوصات الأشعة المقطعية في البطن. تم تقدير ما مجموعه 60 مريضًا بالغًا يخضعون لامتحانات التصوير المقطعي المحوسب بالبطن باستخدام CTDIvol ، وطول الجرعة (DLP) والجرعة الفعالة (E) وتقييم الجرعة الفعالة وجرعة الأعضاء باستخدام برنامج CT expo version 2.5.

أظهرت نتائج هذه الدراسة أن متوسط الجرعة الفعالة للبطن في المستشفى (A) ، والمستشفى (B) والمستشفى (C) كان (7.6) mSv، mSv (5.3) و (6.3) mAs على التوالي. كان معدل DLP للمستشفى (A) ، والمستشفى (B) ، والمستشفى (mGy * cm (450) (C، mGy * cm (410.95) و (380) mGy * سم على التوالي. كان متوسط CTDIvol للبطن في المستشفى (A) ، والمستشفى (B) والمستشفى (mGy (9.9) (C، mGy (8.8) و (7.3) mGy على التوالي وكشفت نتائج هذه الدراسة أن الجرعة المكافئة المتوسطة لأعضاء البطن ، كانت المعدة (12.23) ملي سيفرت ، الطحال (11.99) ملي سيفرت ، كان البنكرياس (9.8) ملي سيفرت والغدة الكظرية (9.158) ملي سيفرت.

والمعلمات (CTDI) تم تقدير جرعات أعضاء المريض باستخدام قياسات مؤشرات الجرعة المقطعية ولوحظ اختلاف .NRPB على أساس عوامل تحويل ImPACT المتعلقة بالتعرض ، وجدول بيانات مماثلة. وقد نشأت هذه الاختلافات إلى CT خفيف من جرعات الجهاز بين المستشفيات الثلاثة لفحوصات حد كبير من بروتوكولات مختلفة لفحص الأشعة المقطعية المستخدمة في المستشفيات الثلاثة المختلفة. جرعات الجهاز في هذه الدراسة

Table of contents

الآية	II
Dedication	III
Acknowledgements	IV
Abstract	V
المستخلص	VI
Table of contents	VII
Chapter One – Introduction	VII
Chapter Two - Theoretical Background	VII
Chapter Three - Materials & Method	VIII
Chapter Four – Results	IX
Chapter five - Discussion, Conclusion and Recommendations	IX
List of Figures	X
List of Abbreviations	XI
List of Tables	XIV

Chapter One – Introduction	
1.1.Introduction	**1**
1.2. Problem of Study	***2***
1.3. Objective	***2***
1.3.1. General Objective	***2***
1.3.2. Specific Objective	***2***
1.4. Outline of the study	***3***

Chapter Two - Theoretical Background	
2.1. Computed Tomography Imaging	**4**
2.2. CT generations	**4**
2.2.1. First Generation: Rotate/translate, Pencil beam	**5**
2.2.2. Second Generation: Rotate/translate, Narrow Fan Beam	**6**
2.2.3. Third Generation: Rotate/Rotate, Wide Fan Beam	**8**
2.2.4. Fourth Generation (Rotate/Stationary)	**9**
2.2.5. Fifth Generation (Stationary/Stationary)	**10**
2.2.6. Sixth Generation: Helical	**12**
2.2.7. Seven Generation: Multiple Detector Array	**13**
2.3. Components of the CT scan	**15**
2.3.1. Gantry and table	**15**
2.3.2 The X ray tube and generator	**15**
2.3.3. Collimation and filtration	**15**
2.3.4. Detectors	**16**
2.4. Dosimetric Quantities and Units	**17**

2.4.1. Basic Dosimetric Quantities	**17**
2.4.1.1. Particle Number N	**17**
2.4.1.2. Radiant Energy R	**17**
2.4.1.3. Fluence Φ	**17**
2.4.1.4. Energy fluence ψ	**17**
2.4.1.5. Kerma K:	**17**
2.4.1.6. Energy imparted	**18**
2.4.1.7. Absorbed Dose D	**18**
2.5. Justification and Optimization of Protection in CT	**19**
2.6. Quantities for CT dosimetry	**20**
2.6.1. Computed Tomography Dose Index CTDI	**20**
2.6.2.Calculating CTDI:	**20**
2.6.3. $CTDI_{FAD}$	**21**
2.6.4. $CTDI_{100}$	**22**
2.6.5. Weighted$CTDI_W$	**23**
2.6.6. Volume $CTDI_{VOL}$	**23**
2.6.7. Dose Length Product DLP	**24**
2.7. Radiation Quantities	**25**
2.7.1. Organ and Tissue Dose D_T	**25**
2.7.2. Equivalent dose H_T	**26**
2.7.3. Effective dose E	**27**
2.7.3.1 Effective Dose E in CT	**29**
2.8. Literature review	**32**

Chapter Three - Materials & Method	
3.1. Materials	**37**
3.1.1 Machines	**37**
3.1.2. Population	**37**
3.2. Methods	**38**
3.2.1. Data Collection	**38**
3.2.2 Dosimetric calculations	**39**
3.1.3.CT-Expo V 2.5 software	**39**
3.3.In put steps	**41**
3.5.Data Analysis	**43**

Chapter Four – Results	
4.1. Results	**44**

Chapter five - Discussion, Conclusion and Recommendations	
5.1. Discussion	**54**
5.2. Conclusion	**56**
5.3. Recommendations	**57**
References	**58**
5.4 Appendix	**60**

List of figures

Figures No	Item	Page NO
2.1	First generation scanners used translation and rotation.	5
2.2	Second generation CT scanner. Rotation-translation of a narrow fan beam.	7
2.3	Third generation CT scanner. Rotation of a wide fan beam	9
2.4	Fourth generation CT scanner. Rotation-fixed with closed detector ring.	10
2.5	Fifth generation CT scanner (Electron beam scanner).	11
2.6	Sixth generation CT scanner (Helical CT).	13
2.7	A comparison between the linear arrays used in other CT generations (A) and the multiple detector array used in the seventh generation CT scanner (B).	14
2.8	Pencil Ion chamber	20
2.9	Calculate D(z)	21
2.10	Phantom and pencil chamber	21
2.11	Length Product	24
2.12	Bar graph shows tissue-weighting factors specified by International Commission on Radiological Protection (ICRP) publications 26, 60, and 103.	29
3.1	Compare the female and male in three hospitals	38
3.2	CT –Expo v2.5	39
3.3	mathematical phantom (ADAM, EVA)	40
3.4	Scan parameter	42
3.5	Results	42
3.7	Organ dose	43
4.1	The average equivalent dose per mSv for some organs during abdomen Ct examination	48
4.2	Compare the equivalent dose per mSv for stomach between three hospitals (A-B-C) during CT examination	48
4.3	Compare the equivalent dose per mSv for spleen between three hospitals (A-B-C) during CT examination	49
4.4	Compare the equivalent dose per mSv for pancreas between three hospitals (A-B-C) during CT examination	49
4.5	Compare the equivalent dose per mSv for adrenals between three hospitals (A-B-C) during CT examination	50
4.6	compare the $CTDI_{vol}$ between three hospitals (A-B-C)	50

4.7	compare the DLP between three hospitals (A-B-C)	**51**
4.8	compare the effective dose (E) between three hospitals (A-B-C)	**51**
4.9	show that the dose presented (CTDI $_{vol}$)	**52**
4.10	show that the dose presented (DPL)	**53**
4.11	show that the dose presented (E)	**53**

List of Abbreviations

CT	*Computed Tomography*
ALARA	*As Low As Reasonably Achievable*
ICRP	*International Commission on Radiological Protection*
DRLs	*diagnostic reference dose levels*
QA	*Quality assurance*
CAT	*Computerized axial tomography*
DAS	*Data Acquisition System*
MSAD	*Multiple Scan Average Dose*
MDCT	*Multi Detector Computed Tomography*
CTDI	*Computed Tomography dose index*
$CTDI_{100}$	*Computed Tomography dose index, for a100 mm length pencil ion chamber*
CTDIvol	*Volumetric Computed Tomography dose index*
CTDIw	*Weighted Computed Tomography dose index*
DLP	*Dose Length Product*
E	*Effective Dose*
D	*Absorbed Dose*
FDA	*Food and Drug Administration*
WR	*Radiation Weighting Factor*
WT	*Tissue Weighting Factor*
KERMA	*Kinetic Energy Released per unit Mass*
Kvp	*Kilo Voltage Peak*
mAs	*Mile Ampere Second*
NRPB	*National Radiological Protection Board*
D_T	*Organ Dose*
H_T	*Equivalent Dose*
MeV	*Mega electron Volt*

mSv	*Mile Sievert*
EC	*European Commission*
NRPB	*National Radiological Protection Board*
ImPACT	*Impact CT patient dosimetry calculator*
AEC	*Automatic Exposure Control*

List of Tables

Table NO	*Item*	*Page NO*
2.1	*Geometry and Historical of CT*	**14**
2.2	*Radiation Weighting Factors WR*	**27**
2.3	*Tissue-Weighting Factors ($WR_)$ for International Commission on Radiological Protection (ICRP) Publications 26, 60, and 103*	**28**
3.1	*Patient population of the study classified per hospital and type of examination.*	**38**
4.1	*Summaries the characteristic performance parameters for the CT systems and console displayed form The CT scanner G E model Acquilion (16-slice) hospital A*	**44**
4.2	*Summaries the characteristic performance parameters for the CT systems and console displayed form The CT scanner G E model Acquilion (16-slice) hospital B*	**45**
4.3	*Summaries the characteristic performance parameters for the CT systems and console displayed form The CT scanner G E model Acquilion (16-slice) hospital C*	**45**
4.4	*The estimation of mean $CTDI_W$, $CTDI_{vol}$, DLP and effective dose calculated by software expo 2.5 were used data collection form CT scanner G E model Acquilion (16-slice) hospital A*	**46**
4.5	*The estimation of mean$CTDI_W$, $CTDI_{vol}$, DLP and effective dose calculated by software expo 2.5 were used data collection CT scanner G E model Acquilion (16-slice) hospital B*	**46**
4.6	*The estimation of mean$CTDI_W$, $CTDI_{vol}$, DLP and effective dose calculated by software expo 2.5 were used data collection CT scanner G E model Acquilion (16-slice) hospital C*	**47**
4.7	*The average equivalent dose per mSv for some organs during abdomen CT examination*	**47**
4.8	*show the mean of CTDI, DLP and E in this study and compare with other country and EC reference dose*	**52**

Chapter One

Introduction

1.1. INTRODUCTION:

Computed Tomography (CT) is a radiologic modality that provides clinical information in the detection, differentiation, and demarcation of disease. It is the primary diagnostic modality for a variety of presenting problems and is widely accepted as a supplement to other imaging techniques. CT is a form of medical imaging that involves the exposure of patients to ionizing radiation.(Ahmad, 2017).During a CT scan a rotating source passes x-rays through a patient's body to produce several cross-sectional images of a particular area. These two-dimensional images can also be digitally combined to produce a single three-dimensional.(Ali, 2005)

Computed tomography (CT) developed from an x ray modality that was limited to axial imaging of the brain in neuroradiology into a versatile 3-D whole body imaging modality for a wide range of applications, including oncology, vascular radiology, cardiology, traumatology and interventional radiology. CT is applied for diagnosis and follow-up studies of patients, for planning of radiotherapy, and even for screening of healthy subpopulations with specific risk factors(Dance et al., 2014a).

CT is an important and sometimes life-saving tool for diagnostic medical examinations and guidance of interventional and therapeutic procedures. It allows rapid acquisition of high-resolution three-dimensional images, providing radiologists and other physicians with cross-sectional views of the patient's anatomy. CT can be used to image many types of tissues, such as soft tissues, bones, lungs, and blood vessels. CT examinations are also non-invasive, although a contrast agent is sometimes administered to the patient. As a consequence of the benefits of CT examinations, it has become the gold standard for a variety of clinical indications, such as diagnosing certain cancers,

surgical planning, and identifying internal injuries and bleeding in trauma cases(Association, 2006).

Diagnostic importance of CT examinations is outstanding, so the increase of examination frequency is justified(Ali, 2005).

According to the International Commission on Radiological Protection (ICRP) dose limits should not be applied for medical exposures either diagnostic or therapy, because patients have direct benefit from the exposure. However according to the basic principles of radiation protection the medical diagnostic procedures should be optimized and unjustified exposures should be minimized(Ali, 2005).

CT procedures give patients more radiation dose than traditional x-ray imaging modalities. Patients are exposed to more dose which may result in unintended heal the effects healthcare providers need to be able to estimate and track the dose these patients Receive from their CT scan(Prins et al., 2011).

1.2. Problem of Study:

Due to use CT scanning patients are exposed to doses which may result in unintended health effects, especially for abdomen become it has very sensitive organs such as adrenal gland - stomach – spleen - pancreas to avoid unnecessary of high dose to the patient need to estimate the effective dose.

1.3. Objectives:

1.3.1. General Objective:

To estimate the effective dose (E) during abdomen CT examination for abdomen organs for (CT SCAN) using CT. Exp version 2.5 software

1.3.2. Specific Objectives:

- To compare Volume Computed Tomography Dose Index ($CTDI_{vol)}$
- To compare Dose Length Product (DLP)
- To calculate Organ equivalent dose (H_T)
- Effective dose (E) for stomach- spleen- and pancreas

1.4. Outline of the study:

Chapter one: This chapter is general introduction to the computed tomography and represents the goal of calculate patient dose. The published literature and studies done on the research subject were reviewed in this chapter to know about bases and methods of assessing the patient dose. The objectives of this study were also mentioned in this chapter.

Chapter two: This chapter explores the computed tomography, hardware of CT, dosimetric quantities and units, quantities related to stochastic and deterministic effect.

Chapter three: This chapter describes the materials and methods used in this research to assess the effective patient dose.

Chapter four: This chapter consists of: presentation of the results in tables.

Chapter five: Introduce the conclusion that had been derived out from the research

Chapter Two

Theoretical Background

2.1. Computed Tomography:

2.2. Geometry and Historical Development:

Computed tomography (CT) is an imaging procedure that uses special X - Ray equipment to create detailed pictures, or scans, of areas inside the body. It is also called computerized tomography and computerized axial tomography (CAT). The term *tomography* comes from the Greek words *tomos* (a cut, a slice, or a section) and *graphein* (to write or record). Each picture created during a CT procedure shows the organs, bones, and other tissues in a thin "slice" of the body. The entire series of pictures produced in CT is like a loaf of sliced bread—you can look at each slice individually (2-dimensional pictures), or you can look at the whole loaf (a 3-dimensional picture). Computer programs are used to create both types of pictures. Most modern CT machines take continuous pictures in a helical (or spiral) fashion rather than taking a series of pictures of individual slices of the body, as the original CT machines did. Helical CT has several advantages over older CT techniques: it is faster, produces better 3-D pictures of areas inside the body, and may detect small abnormalities better. The newest CT scanners, called multi slice CT or multi detector CT scanners, allow more slices to be imaged in a shorter period of time. Computed tomography (CT) is in its fourth decade of clinical use and has proved invaluable as a diagnostic tool for many clinical applications, from cancer diagnosis to trauma to osteoporosis screening. CT was the first imaging modality that made it possible to probe the inner depths of the body, slice by slice. Since 1972, when the first head CT scanner was introduced, CT has matured greatly and gained technological sophistication. Concomitant changes have occurred in the quality of CT Images. The first CT scanner, an EMI Mark 1, produced images with 80 X 80 pixel resolution (3-mm pixels), and each pair of slices required approximately 4.5 minutes of scan time and 1.5 minutes of reconstruction time(Bushberg et al., 2003).

2.2.1. First Generation: Rotate/translate, Pencil beam:

Godfrey Hounsfield developed the first CT scanner in the mid 1970's with the help of a company called Electric and Musical Industries Ltd, the first CT scanners were solely for head scans and used a rotate/translate system with a single x-ray beam called a pencil beam. The pencil beam used parallel beam geometry. In order to produce such a narrow beam of x-ray photons, the first generation scanner used a pinhole collimator to ensure only a single beam of x-rays was interacting with the patient.

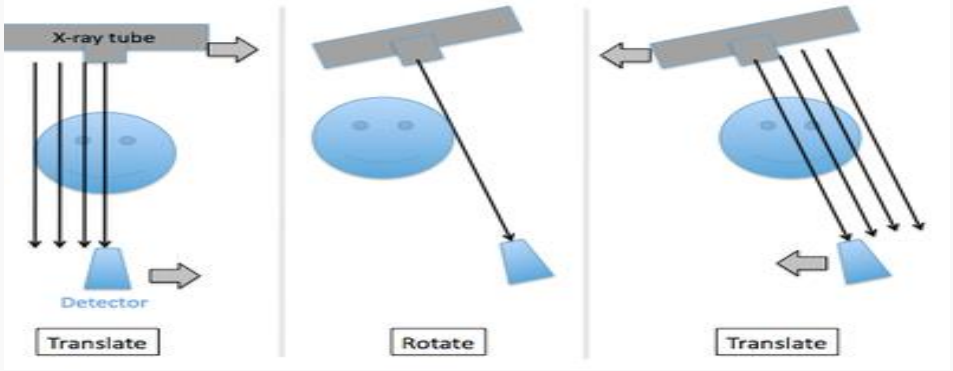

Figure (2.1). First generation scanners used translation and rotation. The x-ray tube and detector translate across one slice (left), then rotates a very small amount (middle), and then translates back across (right). (Figure derived from source 1).

In addition, the first generation CT scanner was made up of only two x-ray detectors, which were located on the opposite side of the patient from where the x-ray tube was situated. This meant that the two detectors were capable of measuring the amount of x-rays that successfully passed through the patient for only two slices of that body part. In order to acquire every slice across a part of the body, the x-ray tube and detectors has to be moved linearly, before rotating the position of the x-ray tube to acquire images at a different projection angle. Therefore, acquiring the CT images required both the detector and the x-ray tube to be physically moved through each of the necessary positions. Due to the required rotation and translation of both the x-ray tube and the detectors, the

first generation CT scanner is often simply classified as the rotation-translation of a pencil beam (Figure 1).

One of the largest advantages associated with the first generation CT scanner was the use of the pencil beam x-ray geometry. Because only two detectors were being used to measure the amount of the x-ray beam that penetrated the body, there was a significant decrease in the amount of scatter radiation interacting with the detectors. This was due to the fact that the small detectors rarely detected any scattered radiation. Therefore, the first generation CT scanners were powerful in terms of scatter reduction.

A major drawback of the first generation CT scanner was the amount of time it took to acquire the images and to reconstruct the images using the computer. This process was very demanding in terms of both time and manpower(Bushberg et al., 2003).

For example, to acquire a full image of the head, the x-ray tube needed to be placed at a certain angle and the x-ray tube and detectors were translated linearly to acquire multiple two-dimensional projections. Then, once approximately 160 separate projections were acquired at that specific projection angle, the x-ray tube and detectors were rotated by one degree and the linear translation commenced again. This process was repeated until all the two-dimensional projection images were acquired at 180 different projection angles.(Bushberg et al., 2003)

2.2.2. Second Generation: Rotate/translate, Narrow Fan Beam:

In hopes of decreasing the amount of time it took to acquire a head CT, the first enhancement to the CT scanner was the incorporation of a narrow fan x-ray beam with an angle of approximately 10 degrees resulting in a linear array of 30 detectors, a major change from the pencil beam and two detectors seen in the first generation (Figure 2). The largest advantage associated with the second generation CT scanner was the substantial decrease in acquisition time compared to that of the first generation. Although the angle of the fan beam was

not large and still required the linear movement of the x-ray tube and detectors at each projection angle, the amount of linear displacement required was dramatically reduced. In fact, the acquisition time for a head CT scan decreased by two to three minutes per slice. Consequently, this generation of CT scanners was measured to be fifteen times faster than the first generation, which has been deemed a massive improvement.

One of the problems associated with the second generation CT scanners was that narrow fan beams, unlike the pencil beam geometry, contribute to scattering. With an increased number of detectors introduced into the system (to compensate for the wider x-ray beam), the detectors were exposed to more scattered radiation decreasing the resolution in the images that were being produced.

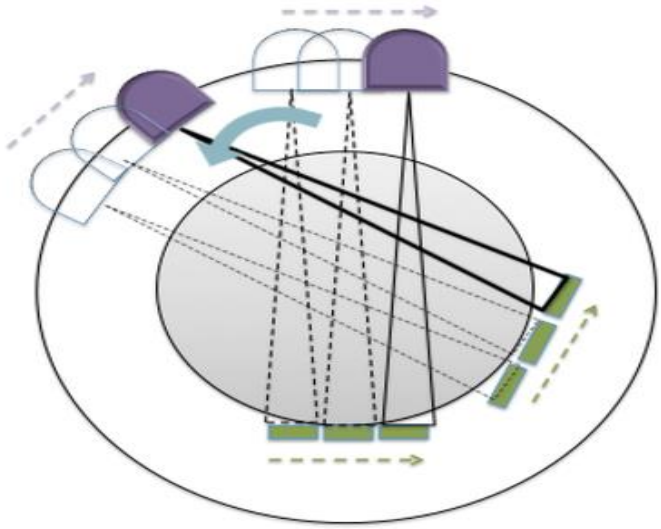

Figure (2.2). Second generation CT scanner. Rotation-translation of a narrow fan beam.

Although it seems like a contradiction, another problem associated with the second generation CT scanner was related to the amount of time it took to acquire images. While the acquisition time improved between the first and second generations, the measuring field in the second generation scanners was still relatively small. This generation still required the rotation and translation of the x-ray tube and detectors, which immediately added unnecessary time to the imaging protocol. For this reason, both the first and second generation CT

scanners were only used to image the head and brain due to its size and limited movement. Parts of the body such as the abdomen and thorax, however, contain constantly moving organs. These intrinsic movements caused many problems when attempting to acquire images, particularly in terms of the development of artifacts on the reconstructed images (Bushberg et al., 2003)

2.2.3. Third Generation: Rotate/Rotate, Wide Fan Beam:

Translational motion, which was used in first- and second-generation scanners, was quite time consuming. At this stage in development, the main goal was to cut the acquisition time to less than 20 seconds so that the brain could be imaged more rapidly, but also so that physicians could image parts of the body other than the head. The goal of 20 seconds was important to the further development of the CT scanner because it meant that someone could hold their breath for images acquisition of the abdomen, reducing artifacts from the lung movement on the reconstructed images. It was suggested that instead of having to linearly translate the x-ray tube and detector system after each change in acquisition angle, it would make more sense to eliminate the translational movements all together. This promoted the introduction of a wide aperture fan x-ray beam, which could reach the entire patient (slice) at one time: this meant that the x-ray tube and the detectors could now rotate freely through each of the projection angles without stopping to collect multiple slices per projection angle. This specifically was what eliminated translational motion in CT.(Bushberg et al., 2003)

The wide aperture fan beam approach of the third generation CT scanner involved an x-ray fan beam with an angle ranging between 40 to 60 degrees. Much like in the second generation, the increase in the angle of the x-ray fan beam required the introduction of a longer linear detector array. This new array consisted of 400 to 1000 detector elements. In order to facilitate the synchronous rotation of the x-ray tube and the detectors, these two parts of the CT scanner were joined so that they could rotate together (hence "Rotate/Rotate", Figure 3), allowing for an even faster acquisition time .

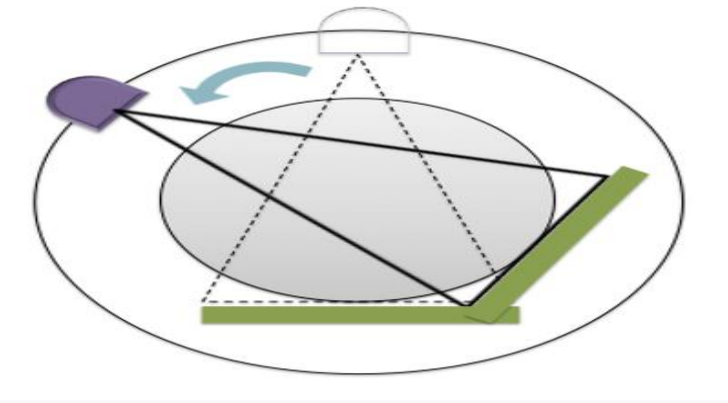

Figure (2.3). Third generation CT scanner. Rotation of a wide fan beam

The greatest advantage of this generation of CT scanners was the large decrease in the amount of time it took to scan a patient. Some systems could deliver scan times of shorter than 5 seconds per projection angle, making the scans very short and easy to tolerate. Nowadays, third generation CT scanners are still in existence, and most offer scan times of half of a second.

The third generation of CT scanners has two major disadvantages:

- Firstly, the addition of 400 to 1000 detector elements is much more expensive than only using two or thirty detector elements. However, it is argued that due to the dramatic decreases in acquisition time, which largely benefits the patient, the extra expense is justified.
- Secondly, third generation CT scanners produce a characteristic *image artifact* known as ring artifacts. These artifacts are produced due to the large number of detectors and the lack of calibration that is often present between the detectors.

2.2.4. Fourth Generation (Rotate/Stationary):

Fourth generation scanners were developed specifically to alleviate the ring artifacts produced by the third generation. Specifically, the impossibility to have such a large array of rotating detector elements (>400) are perfectly synced and calibrated to one another. By removing the detectors from the rotating gantry and putting them in a stationary ring around the patient, detectors were able to

maintain calibration. This stationary 360 degree ring of detectors required an increased number of detector elements (~5000 total) (Figure 2.5). In these systems, the fan-shaped x-ray beams are processed (to construct the image) with individual detectors as the vertex of a fan. This fan beam data is acquired using one detector over the time period it takes for the x-ray tube to rotate from side to side of the fan arc angle. Due to this set-up, fourth generation CT scanners are said to operate using a rotate-stationary geometry.(Bushberg et al., 2003)

Additionally, it is important to note that the x-ray tube can rotate either outside or inside the detector ring. If the x-ray tube rotates outside of the detector ring, it is crucial that the detector ring is tilted so that the x-rays only interact with the detectors once they pass through the patient, not beforehand.

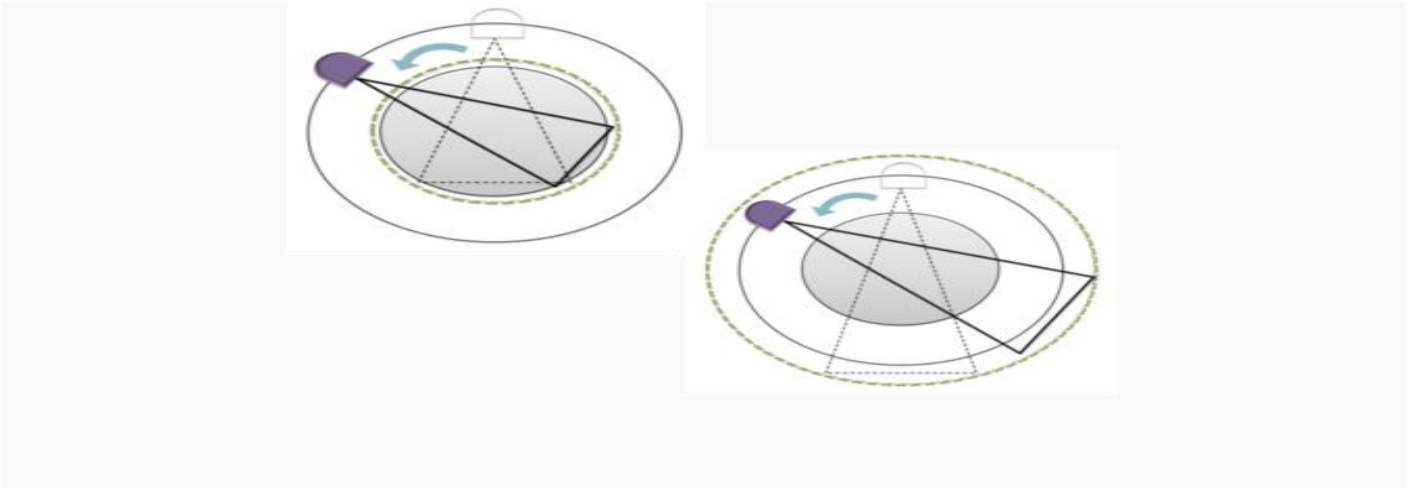

Figure (2.4). Fourth generation CT scanner. Rotation-fixed with closed detector ring. The detectors can be located either inside or outside of the rotation axis of the x-ray tube.

2.2.5. Fifth Generation (Stationary/Stationary):

Fifth generation CT scanners were developed specifically for use in cardiac tomography imaging. These scanners were often referred to as cine-CT scanners, or more commonly electron beam scanners. Up until this point, the

CT scanner had progressed immensely to allow the majority of the body to be imaged. However, it was believed that even shorter acquisition times were required to acquire the best images of the heart due to rapid motion and continual beating.(Bushberg et al., 2003)

Researchers believed that the best way to further decrease the acquisition time was to restrict all motion of the CT scanner components. The fifth generation CT scanner is therefore composed of no moving parts (hence "stationary/stationary"). Instead of the x-ray tube rotation, these electron beam scanners consist of essentially a large x-ray tube inside which the patient lies during the scan. Behind the patient, there is an electron beam, which ejects electrons. This electron beam is electronically deflected down, away from the patient, and makes contact with a large, half-circle tungsten target ring that encircles the patient. The interaction of the electrons with the target ring generates an x-ray beam, which travels through the patient's chest and is detected by a detector ring on the opposite side (Figure 5).

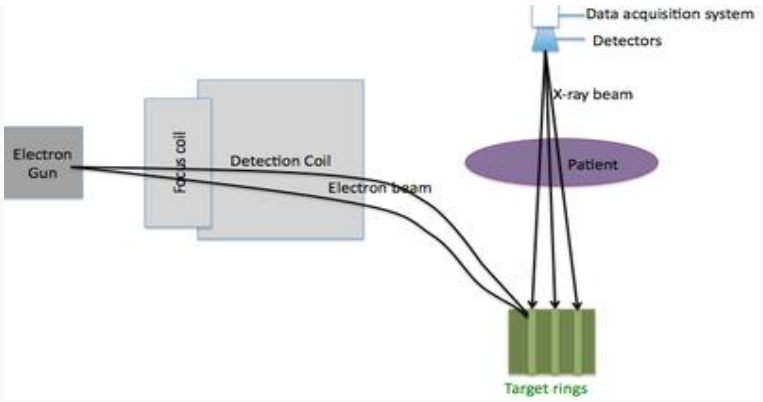

Figure (2.5). Fifth generation CT scanner (Electron beam scanner). Stationary/stationary. The electron beam is directed around the target rings, allowing for all stationary instrumentation

The major advantage of this generation of CT imaging is the fact that it allows for very high-speed image acquisition, ultimately allowing for the production of CT "movies" of the beating heart. Each scan time is about 50 msec and can capture the unique contractions and relaxation of the heart. However, as mentioned, this generation of CT scanner was produced with the intention of imaging specifically the heart and hence was only marketed to cardiologists. Because of this, this generation of CT was very expensive, not very versatile, and ultimately not a very popular addition to the field of medical imaging

2.2.6. Sixth Generation: Helical:

In previous generation detectors, the gantry had to be stopped after ever slice, so that data acquisition could not be a continuous process. Likewise, for image acquisition, it is crucial that energy be constantly supplied to the x-ray tube and the detectors. Therefore, in order to have perpetual access to an energy source, the x-ray tube and the detectors were connected to an electrical source via wires, and had to be stationary; a massive impediment to reducing the amount of time needed to acquire CT images (Bushberg et al., 2003)

This problem was solved in the 1990's when slip ring technology was introduced to the field of medical imaging. A slip ring allows electricity to be passed to rotating components without needing stationary components. Using a slip ring allowed the gantry to rotate continuously through all of the patient slices, therefore creating shorter scan times. This led to the development of the sixth generation CT scanner, also known as helical CT (or, less accurately, spiral CT) (Figure 6).

This generation essentially combined the principles of the third and fourth generations with the slip ring technology to create a system that could rotate continually around the patient without being limited by electrical wires. Above all, the introduction of the slip ring technology to the world of CT permits much shorter acquisition times (i.e., as short as 30 seconds to scan the entire abdomen). The main drawback of helical CT scanners lies in the nature in which the data is collected. Since the data is acquired in a helical formation, no full slices of data are available because the scanner is not producing planar sections. This problem can be compensated for through the reconstruction process.(Bushberg et al., 2003)

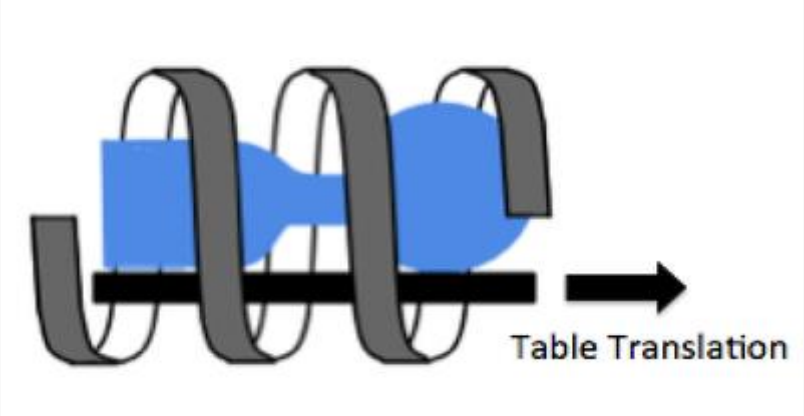

Figure (2.7). Sixth generation CT scanner (Helical CT). X-ray source and detector array rotate continuously as the patient table is moved progressively through the scanner.

2.2.7. Seven Generation: Multiple Detector Array:

The most recent generation of CT scanner consists of a multiple detector array and a cone shaped x-ray beam. Recall that when the CT scanner progressed from the pencil beam geometry to the fan beam geometry, the x-ray beam was used more efficiently. Not only did more of the x-ray beam interact with the detectors, but these wide angled x-ray beams allowed for images to be acquired more rapidly.(Bushberg et al., 2003)

Unlike the pencil beam and fan beam, the cone beam does not pass through a narrow collimator. Therefore, the intensity of the initial x-ray beam is not as strongly reduced and hence can interact more efficiently and effectively with the detector array. In order to use a cone beam x-ray geometry, the linear detector array found in previous generations of CT scanners had to be modified to make a flat panel detector or a multiple detector array. Essentially, the combination of the cone shaped x-ray beam and the paneled detector allows for a very large number of slices to be acquires in a very short period of time (Figure 7). The seventh generation CT scanner can acquire an outstanding amount of information in a very short time span, requiring a much higher level of sophistication in the reconstruction process.

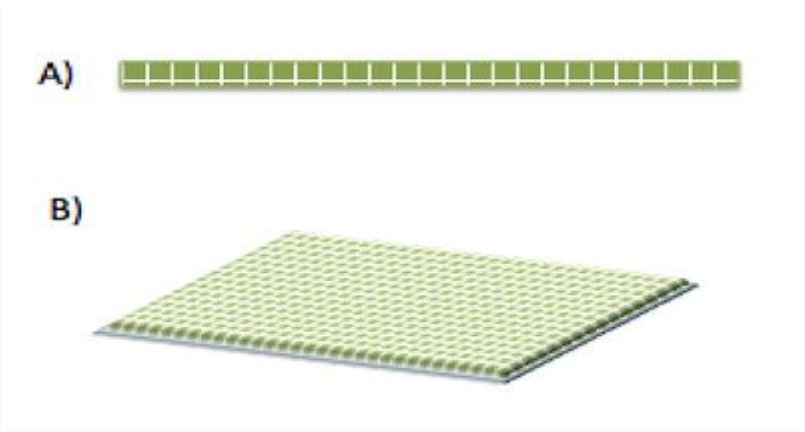

Figure (2.7).: A comparison between the linear arrays used in other CT generations (A) and the multiple detector array used in the seventh generation CT scanner (B).

Table. (2.1): Geometry and Historical of CT

Generation	Source	Source	Detector
1st	Single X-ray Tube	Pencil Beam	Single
2an	Single X-ray Tube	Fan Beam (not enough to cover FOV)	Multiple
3rd	Single X-ray Tube	Fan Beam (not enough to cover FOV)	Many
4th	Single X-ray Tube	Fan Beam covers FOV	Stationary Ring of Detectors
5th	Many tungsten anodes in single large tube	Fan Beam	Stationary Ring of Detectors
6th	3G/4G	3G/4G	3G/4G
7th	Single X-ray Tube	Cone Beam	Multiple array of detectors

2.3. Components of the CT scan

2.3.1. Gantry and table:

The gantry contains all the system components that are required to record transmission profiles of the patient. Since transmission profiles have to be recorded at different angles, these components are mounted on a support within the gantry that can be rotated. The x- ray tube with high voltage generator and tube cooling system, the collimator, the beam shaping filters, the detector arc and the data acquisition system are all mounted on this support. The engineering of these components is complex, since they need to be able to withstand the strong centrifugal force that occurs during the fast rotation of the gantry. Forces of several tens of g arise for rotation times of the order of 0.25 s. electrical power is generally supplied to the rotating gantry by means of slip ring contacts. Recorded projection profiles are generally transmitted from the gantry to a computer by means of wireless communication technologies. The design and engineering of the table, as with the gantry, are critical to allowing accurate acquisition of data at high rotational speeds. The table must also be able to withstand heavy weights without bending. The position of the patient on the table can be head first or feet first, and supine or prone; this position is usually recorded with the scan data(Dance et al., 2014b)

2.3.2. The X- ray tube and generator:

Owing to the high X - ray flux required for CT, the X ray tube uses a tungsten anode designed to withstand and dissipate high heat loads. With long continuous acquisition cycles, a forced cooling system using oil or water circulated through a heat exchanger is often used(Dance et al., 2014b).

2.3.3. Collimation and filtration:

After transmission through the patient, the x-ray beam is collimated to confine the transmission measurement to a slice with a thickness of a few millimeters. Collimation also serves to reduce scattered radiation to less than

1% of the primary beam intensity. The height of the collimator defines the thickness of the CT slice. This height, when combined with the area of a single picture element (pixel) in the display, defines the three dimensional volume element (voxel) in the patient corresponding to the two-dimensional pixel of the display. A voxel encompassing a boundary between two tissue structures (e.g.,) muscle and bone) yields an attenuation coefficient for the pixel that is intermediate between the values for the two structures. This "partial-volume artifact" may be reduced by narrowing the collimator to yield thinner slices. However, this approach reduces the number of x rays incident upon the detector. With fewer x rays interacting in the detector, the resulting signals are subject to greater statistical fluctuation and yield a noisier image in the final display(Dance et al., 2014b).

2.3.4. Detectors:

The essential physical characteristics of CT detectors are a good detection efficiency and a fast response with little afterglow. Currently, solid state detectors are used, as they have a detection efficiency close to 100% compared with high pressure, xenon filled ionization chambers that were used previously and that had a detection efficiency of about 70%. Solid state detectors are generally scintillators, meaning that the x- rays interacting with the detector generate light. This light is converted to an electrical signal, by photodiodes that are attached to the back of the scintillator, which should have good transparency to ensure optimal detection. Typically, an ant scatter grid is mounted at the front of the detector, which consists of small strips of highly attenuating material (e.g. tungsten) aligned along the longitudinal (z) axis of the CT scanner. Detector row consists of thousands of dels that are separated by septa designed to prevent light generated in one Del from being detected by neighboringdels. These septa and the strips of the ant scatter grid should be as small as possible since they reduce the effective area of the detector and thus reduce the detection of x-rays.(Dance et al., 2014b)

2.4. Dosimetric Quantities and Units:

2.4.1. Basic Dosimetric Quantities:

2.4.1.1. Particle Number N:

The particle Number N is the number of particles that are emitted transferred, or received (Dance et al., 2014a).

2.4.1.2. Radiant Energy R:

The Radiant Energy R is the energy (excluding rest energy) of particles that are emitted, transferred, or received.(Dance et al., 2014a)

2.4.1.3. Fluence Φ:

The fluence, Φ, is the quotient dN by da, where dN is the number of particles incident on a sphere of cross-sectional area dA, thus:

$$\Phi = \frac{dN}{dA} \quad \text{---------- (2.1)}$$

The unit of particle Fluence is m-2.(Dance et al., 2014a)

2.4.1.4. Energy fluence ψ:

The energy fluence, Ψ, is the quotient d*R* by d*a*, where d*R* is the radiant energy incident on a sphere of cross-sectional area d*A*, thus: (Dance et al., 2014a)

$$\Psi = \frac{dR}{dA} \quad \text{---------- (2.2)}$$

2.4.1.5. Kerma K:

The kerma, K, is the quotient dEtr by dm, where $d\bar{E}$ is the sum of the initial kinetic energies of all the charged particles liberated by uncharged particles in a mass dm of material, thus:

$$K = \frac{d\bar{E}}{dm} \quad \text{---------- (2.3)}$$

The unit of kerma is joule per kilogram (J/kg). The name for the unit of kerma is the gray

(Gy), where 1 Gy = 1 J/kg (Dance et al., 2014a).

2.4.1.6. Energy imparted:

The mean energy imparted, E –, to the matter in a given volume equals the radiant energy, R_{in}, of all those charged and uncharged ionizing particles which enter the volume minus the radiant energy, R_{out}, of all those charged and uncharged ionizing particles which leave the volume, plus the sum, ΣQ, of all changes of the rest energy of nuclei and elementary particles which occur in the volume, thus:

$$\boldsymbol{E = \sum R_{in} - R_{out} + Q} \qquad \text{---------- (2.4)}$$

Unit: $J \cdot kg^{-1} \cdot s^{-1}$. If the special name gray is used, the unit of kerma rate is gray per second (Gy/s).(Dance et al., 2014a)

For the photon energies used in diagnostic radiology, ΣQ is zero In this Code of Practice, the term 'mean energy imparted' is shortened to 'energy imparted.(Dance et al., 2014a)

2.4.1.7. Absorbed Dose D:

The Absorbed Dose D, is the quotient of dĒ by dm, where dĒ is the mean energy imparted by ionizing radiation to matter of mass dm thus

$$\boldsymbol{D = \frac{d\bar{E}}{dm}} \qquad \text{---------- (2.5)}$$

Unit: J/ Kg

Unit: J/kg. The special name for the unit of absorbed dose is gray (Gy).

In diagnostic radiology, the production of bremsstrahlung within low atomic number materials is negligible. For a given material and radiation field, absorbed dose and kerma are then numerically equal when secondary electron equilibrium is established. There will be important numerical differences between the two quantities wherever secondary electron equilibrium is not

established (i.e. close to an interface between different materials).(Dance et al., 2014a)

2.5. Justification and Optimization of Protection in CT

The principles of radiation protection as stated by ICRP are justification, optimizations of protection and dose limitation(Valentin, 2007)

The principle of dose limitation applies to occupational and public exposure but not for patients. On the other hand, both quality assurance (QA) and diagnostic reference dose levels (DRLs) have been recommended for implementation of the principle of optimizations of protection.(Valentin, 2007)

- Justification: for examinations involving ionizing radiation, such as CT, is an important way of avoiding unnecessary exposure and thus a powerful radiation protection tool. It is widely believed that many unjustified exposures are made both in developing and industrialized countries. Therefore, the referring physician has responsibility for the justification of an examination in individual cases and obtaining the advice of a radiologist for any alternative examination that would provide the desired information.

- Optimization of Protection in X-Ray Computed Tomography: As the medical use of X-ray imaging is clearly justified because the clear benefit that weight radiation, optimization is certainly the most important parameters to consider. In medical imaging optimization include regular dose surveys for audits, applications of DRLs and QA

- Dose Limits: The total dose to any individual from regulated sources in planned exposure situations other than medical exposure of patients should not exceed the appropriate limits specified by the ICRP.(Dance et al., 2014b)

2.6. Quantities for CT dosimetry:

2.6.1. Computed Tomography Dose Index CTDI:

The local tissue dose from a single slice is not the same as the dose in the very same tissue when additional adjacent slices are made, because each additional slice scatters radiation into adjacent slices.(Boone, 2012)

Even if slices are non-overlapping (and ignoring beam penumbra) scatter tails of multiple contiguous scans overlap and contribute to an increased integral dose Profile, which is a Function of:

- Single Scan Profile Width (T)
- Number of scans (N)
- Spacing (I) between slices

- Computed Tomography Dose Index (CTDI) – defined:

2.6.2. Calculating CTDI:

Single axial scan (in phantom to emulate patient scatter) of nominal *beam* thickness T is given by:

$$\boldsymbol{CTDI = \frac{1}{T}\int_{-\infty}^{\infty} D\,(z)dz} \qquad \text{---------- (2.6)}$$

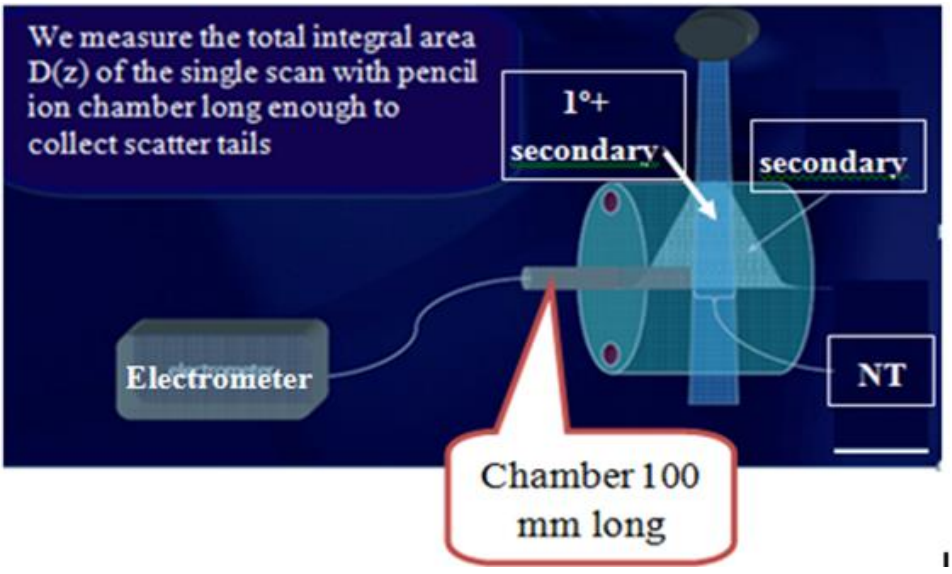

Figure: (2.8) Pencil Ion chamber

D(z) = dose profile along z-axis from:

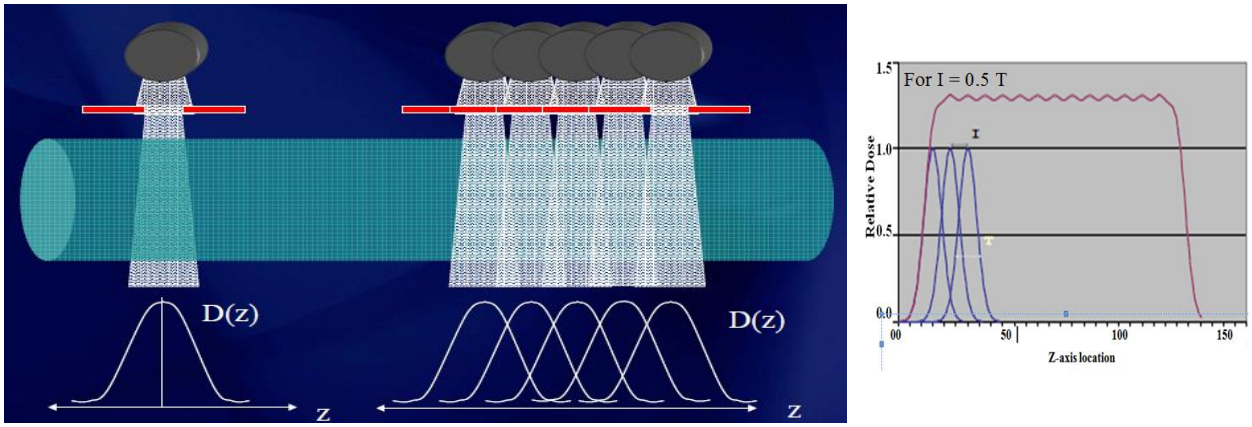

Figure: (2.9) Calculate D(z)

For a number of slices N each thickness T

$$CTDI = (1/NT) \int_{-\infty}^{\infty} D(z)dz$$

CTDI is a good measure of CT x-ray **tube radiation output**, but it does not give patient dose directly, i.e. CTDI and patient dose are not the same.(Boone, 2012) CTDI is a good measure of dose to a 32 cm diameter, 1.19 g/cm^3 piece of plastic (the phantom). Most patients will be smaller, and have higher doses. Larger patients will have lower doses (at the same techniques).(Boone, 2012)

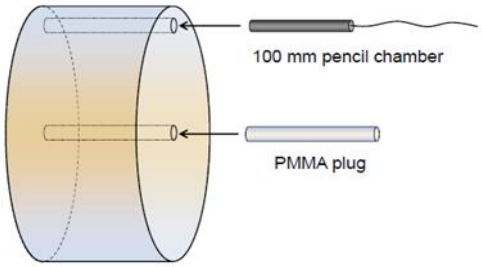

Figure: (2.10).Phantom and pencil chamber

2.6.3. $CTDI_{FAD}$:

Theoretically, the equivalence of the MSAD and the CTDI requires that all contributions from the tails of the radiation dose profile be included in the CTDI dose measurement. The exact integration limits required to meet this criterion depend upon the width of the nominal radiation beam and the

scattering medium. To standardize CTDI measurements (infinity is not a likely measurement parameter), the FDA introduced the integration limits of ±7T, where to represent the nominal slice width Interestingly, the original CT scanner, the EMI Mark I, was a dual detector -row system .Hence, the nominal radiation beam width was equal to twice the nominal slice width (i.e., NxTmm).To account for this, the CTDI value must be normalized to 1/NT:

As described in equ below

$$\boldsymbol{CTDI_{FAD} = \frac{1}{NT}\int_{-7T}^{7T} D(z)dz} \qquad \textbf{---------- (2.8)}$$

2.6.4. $CTDI_{100}$:

CTD100 represents the accumulated multiple scan dose at the center of a 100-mm scan and underestimates the accumulated dose for longer Scan lengths. It is thus smaller than the equilibrium dose or the MSAD. The CTDI100, like the CTDIFAD requires integration of the radiation dose profile from a single axial scan over specific integration limits. In the case of CTDI100, the integration limits are ±50 mm, which corresponds to the 100-mm length of the commercially available "pencil" ionization chamber as described in equ below [8]. When using a chamber of length 10 cm:

$$CTDI = (1/NT)\int_{-50mm}^{+50mm} D(z)dz \qquad \textbf{---------- (2.9)}$$

2.6.6. Weighted$CTDI_W$:

The CTDI varies across the field of view (FOV). For example, for body CT imaging, the CTDI is typically a factor or two higher at the surface than at the center of the FOV. The average CTDI across the FOV is estimated by the Weighted CTDI ($CTDI_W$),

Where

$$\boldsymbol{CTDI_W = {}^{1}/_{3}\, CTDI_{100,center} + {}^{2}/_{3}\, CTDI_{100,edge}} \quad -------- (2.10)$$

The values of 1/3 and 2/3 approximate the relative areas represented by the center and edge values. CTD Wisa useful indicator of scanner radiation output for a specific Kvp and mAs.

2.6.7. Volume $CTDI_{VOL}$:

To represent dose for a specific scan protocol, which almost always involves series of scans, it is essential to take into account any gaps or overlaps between the x-ray beams from consecutive rotations of the X-ray source. This is accomplished with use of a dose descriptor known as the Volume $CTDI_W$ ($CTDI_{VOL}$),

Where

$$\boldsymbol{CTDI_{VOL} = \frac{NT}{I} \times CTDI_W} \quad \textbf{---------- (2.11)}$$

Where: I = the table increment per axial scan (mm) Since the pitch is define as the ratio of the table travel per rotation (I) to the total nominal beam width (N×T)

$$\textbf{Pitch} = \boldsymbol{\frac{1}{T \times N}} \quad \textbf{---------- (2.12)}$$

Thus, the volume CTDI can expressed as

$$\boldsymbol{CTDI_{VOL} = \frac{CTDI_W}{pitch}} \quad \text{---------- (2.13)}$$

Whereas $CTDI_W$ represents the average absorbed radiation dose over the *x* and *y* directions at the center of the scan from a series of axial scans where the scatter tails are negligible beyond the 100-mm integration limit, $CTDI_{vol}$represents the average absorbed radiation dose over the*x*, *y*, and *z* directions.

The $CTDI_{vol}$ provides a single CT dose parameter, based on a directly and easily measured quantity, which represents the average dose within the scan volume for a standardized (CTDI) phantom. The SI units are milligray (mGy).

2.5.8. Dose Length Product DLP:

To better represent the overall energy delivered by a given scan protocol, the absorbed dose can be integrated along the scan length to compute the Dose-Length Product (DLP) where *DLP* (mGy-cm) = *CTDI*vol (mGy) x *scan length* (cm).

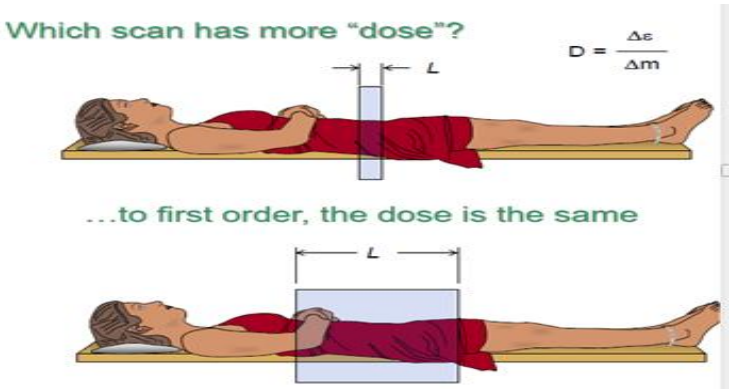

Figure: (2.11) Length Product

The DLP reflects the total energy absorbed (and thus the potential biological effect) attributable to the complete scan acquisition. Thus, an abdomen-only CT exam might have the same $CTDI_{vol}$ as an abdomen and pelvis CT exam, but the latter exam would have a greater DLP, proportional to the greater *z*-extent of the scan volume. Thus, probability of stochastic effect depends on both dose and volume (length) irradiated, hence the principle Dose Length Product [DLP]:

DLP = CTDI × L mGy.cm ---------- (2.14)

DLP = ($CTDI_w$), T.N.C mGy.cm --------- (2.15)

Where: N number of slices

T (cm) thickness of each slice

C (mAs) radiographic exposure.

L =T.N.C

The DLP reflects the total energy absorbed (and thus the potential biological effect) attributable to the complete scan acquisition. Thus, an abdomen-only CT exam might have the same **$CTDI_{vol}$** as an abdomen/pelvis CT exam, but the latter exam would have a greater DLP, proportional to the greater *z*-extent of the scan volume(Hassan, 2012).

2.7. Radiation Quantities

The absorbed dose is the basic physical dosimetry quantity, but it is not entirely satisfactory for radiation protection purposes because the effectiveness in damaging human tissue differs for different types of ionizing radiation. In addition to the physical quantities, other dose related quantities have been introduced to account not only for the physical effects but also for the biological effects of radiation upon tissues. These quantities are organ dose, equivalent dose, effective dose, committed dose and collective dose.(Podgorsak, 2005)

2.7.1. Organ and Tissue Dose D_T:

The equivalent dose, H_T, to an organ or tissue, T, is defined in ICRP 60 and ICRU 51. For a single type of radiation, R, it is the product of a radiation weighting factor W_R, for radiation R and the organ dose, D_T, thus:

$$\mathbf{D_T = \frac{E_T}{m_T}} \quad \text{---------- (2.16)}$$

Unit: J/kg. The special name for the unit of equivalent dose is Sievert (Sv).

The radiation weighting factor, W_R, allows for differences in the relative biological effectiveness of the incident radiation in producing stochastic effects at low doses in tissue or organ, T. For X ray energies used in diagnostic radiology, W_R is taken to be unity.(Dance et al., 2014b)

2.7.2. Equivalent dose H_T:

The equivalent dose, HT, to an organ or tissue, T, is defined in ICRP 60 [3.13] and ICRU 51 [3.11]. For a single type of radiation, R, it is the product of a radiation weighting factor, W_R, for radiation R and the organ dose, DT, thus:

$$\mathbf{H_T = W_R \; X \; D_T} \qquad \text{---------- (2.17)}$$

Unit: J/kg. The special name for the unit of equivalent dose is sievert (Sv).

The radiation weighting factor, W_R, allows for differences in the relative biological effectiveness of the incident radiation in producing stochastic effects at low doses in tissue or organ, T. For X ray energies used in diagnostic radiology, W_R is taken to be unity.(Dance et al., 2014b)

Table (2.2): Radiation Weighting Factors W_R

Radiation	Weighting Factors
Photons all energies	**1**
Electrons and muons, all energies	**1**
Neutrons	
< 10 Kev	**2.5**
10 – 100 Kev	**2.5 to 10**
100 – 2 Mev	**10 to 20**
2 – 20 Mev	**7 to 17.5**
>20Mev	**5 to 7**
Protons, energy > 2 Mev	**2**
Alpha particles, fission fragment, heavy nuclei	**20**

2.7.3. Effective dose E:

The effective dose, E, is defined in ICRP 60 [3.13] and ICRU 51 [3.11]. It is the sum over all the organs and tissues of the body of the product of the equivalent dose, HT, to the organ or tissue and a tissue weighting factor, W_T, for that organ or tissue, thus:

$$\boldsymbol{E = \sum W_T H_T} \quad \text{---------- (2.18)}$$

The tissue weighting factor,$W_{T,}$ for organ or tissue T represents the relative contribution relative contribution of that organ or tissue to the total detriment arising from stochastic effects for uniform irradiation of the whole body.

Unit: J/Kg. The special name for the unit of effective dose is Sievert (Sv)(Dance et al., 2014b).

TABLE (2.3): Tissue-Weighting Factors (W_T) for International Commission on Radiological Protection (ICRP) Publications 26, 60, and 103

Tissue	**Weighting Tissue , W_T**
Gonads	**0.8**
Breast	**0.12**
Red bone marrow	**0.12**
Lung	**0.12**
Thyroid	**0.04**
Bone surface	**0.01**
Colon	**0.12**
Stomach	**0.12**
Bladder	**0.04**
Esophagus	**0.04**
Liver	**0.04**
Brain	**0.01**
Kidney –	**-**
Salivary glands	**0.01**
Skin	**0.01**
Remainder	**0.12**

The remainder is composed of the following additional tissue and organs: adipose tissue, adrenals, connective tissue, extra thoracic airways, gall bladder, heart wall, kidney, lymphatic nodes, muscle, pancreas, prostate, small intestine wall, spleen, thymus and uterus/cervix

$$\boldsymbol{E = k \times DLP} \text{ ---------- } (2.19)$$

Where the *k* coefficient (Table 2.3) is specific only to the anatomic region scanned.

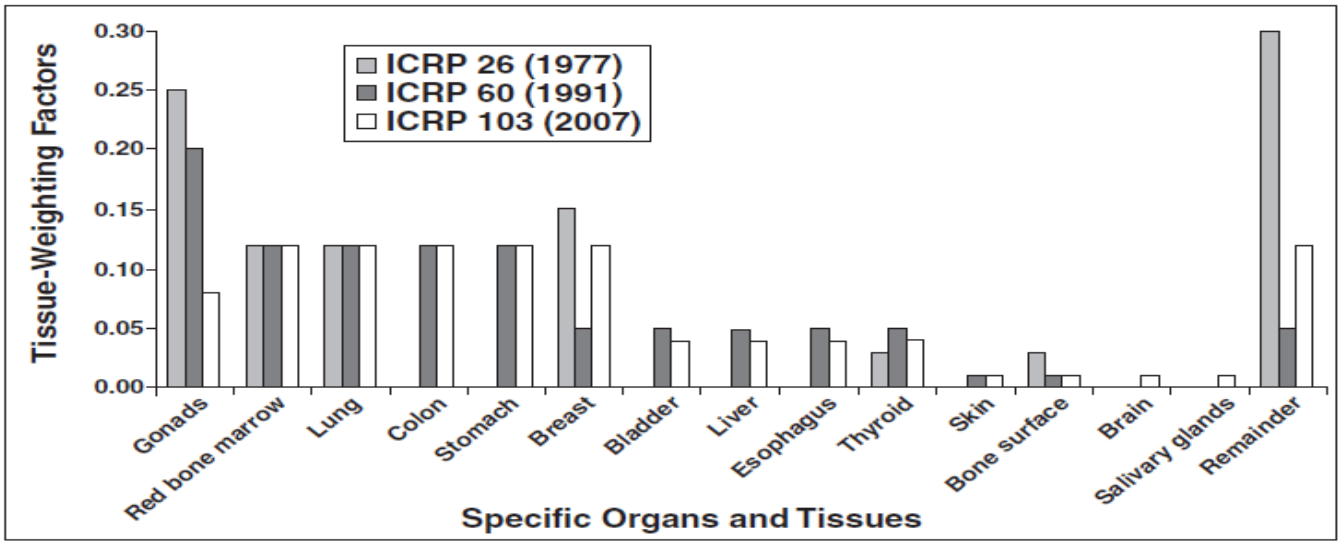

Figure (2.12) Bar graph shows tissue-weighting factors specified by International Commission on Radiological Protection (ICRP) publications 26, 60, and 103.

2.7.3.1 Effective Dose E in CT:

It is important to recognize that the potential biological effects from radiation depend not only on the radiation dose to a tissue or organ, but also on the biological sensitivity of the tissue or organ irradiated. A 100-mGy dose to an extremity would not have the same potential biological effect (detriment) as a 100-mGy dose to the pelvis. Effective dose, E, is a dose descriptor that reflects this difference in biologic sensitivity. It is a single dose parameter that reflects the risk of a non-uniform exposure in terms of an equivalent whole-body exposure. The units of effective dose are Sievert (usually millisievert (mSv) are used in diagnostic radiology). The concept of effective dose was designed for radiation protection of occupationally exposed personnel. It reflects radiation detriment averaged over gender and age, and its application has limitations when applied to medical populations. However, it does facilitate the comparison of biologic effect between diagnostic exams of different types. The use of effective dose facilitates communication with patients regarding the potential harm of a medical exam that uses ionizing radiation. Characterizing the radiation dose in terms of effective dose and comparing that value to other radiation risks, for instance, one year's effective dose from naturally occurring background radiation, better conveys to the patient the relative potential for

harm from the medical exam. It is important to remember, however, that the effective dose describes the relative “whole body” dose for a particular exam and scanner, but is not the dose for any one individual. Effective dose calculations use many assumptions, including a mathematical model of a “standard” human body that does not accurately reflect any one individual (it is and erogenous and of an age representative of a radiation worker). Effective dose is best used to optimize exams and to compare risks between proposed exams. It is a broad measure of risk, and as such, should not be quoted with more than one or two significant digits. The most direct way of estimating doses to patients undergoing CT examinations is to measure organ doses in patient-like phantoms. Another way of obtaining the pattern of energy deposition in patients undergoing CT examinations is by calculation. Computations that use Monte Carlo methods follow the paths of a large number of x-rays as they interact with a virtual phantom and estimate the probability of the dominant interaction processes (i.e., Compton scatter and photo electric absorption). This type of calculation assumes that the patient resembles the phantom used for measurements or Monte Carlo simulation. When patients differ in size and composition, appropriate corrections might need to be used. The resultant information is the absorbed dose to a specified tissue, which may be used to predict the biological consequences to that (single) tissue. CT examinations, however, irradiate multiple tissues having different radiation sensitivities. The effective dose takes in to account how much radiation is received by an individual tissue, as well as the tissue’s relative radiation sensitivity. Specific values of effective dose can be calculated using several different software packages, which are based on the use of data from one of two sources, the National Radiological Protection Board (NRPB) in the United Kingdom or the Institute of Radiation Protection (GSF) in Germany. A free Excel spreadsheet can be downloaded from organ dose and effective dose estimates using the (NRPB) organ dose coefficients. Other packages are available for purchase. To minimize controversy over differences in effective dose values that are purely the result of calculation methodology and data sources, a generic estimation

method was proposed by the European Working Group for Guidelines on Quality Criteria in Computed Tomography. Effective dose values calculated from the NRPB Monte Carlo organ coefficients were compared to DLP values for the corresponding clinical exams to determine a set of coefficients k, where the values of k are dependent only on the region of the body being scanned (head, neck, thorax, abdomen, or pelvis). Using this methodology, E can be estimated from the DLP, which is reported on most CT systems: The values of E predicted by DLP and the values of E estimated using more rigorous calculations methods are remarkably consistent, with a maximum deviation from the mean of approximately10% to 15%. Hence, the use of DLP to estimate E appears to be a reasonably robust method for estimating effective dose. Similarly, Huda has compared effective dose, as calculated from the NRPB data, to estimates of energy imparted in order to develop conversion coefficients by which to later estimate effective dose from energy imparted(Huda et al., 2011).

2.8. Literature review:

L. sadri et al, (Sadri et al., 2013) presented result of assessed and evaluated patient radiation doses for adults common examination to derive local diagnostic guidance level for common CT examination performed in Volume and weighted computed tomography dose index ($CTDI_{VOL}$, W) and dose length product (DLP) of four common CT examinations including head, head sinus, chest, abdomen and pelvis were measured for 8 different CT scanners using standard head and body phantoms. The image quality of acquired scan images was assessed according to European Commission (EC) image quality criteria guidelines. The results of them study were shown more patient doses in terms of DLP for head sinus in compare with other studies while $CTDI_W$ values for head base and sinus were higher than EC measurements. The great variations of $CTDI_W$ and DLP observed among hospitals and relatively high values of DLP in some centers are evidence that radiation doses of patients from CT examinants is not fully optimized.

Justin E et al, (2006) reported of Estimation of patient organ doses from CT examinations in Tanzania. The aims of this study are, first, to determine the magnitude of radiation doses received by selected radiosensitive organs of patients undergoing CT examinations and compare them with other studies, and second, to assess how CT scanning protocols in practice affect patient organ doses. In order to achieve these objectives, patient organ doses from five common CT examinations were obtained from eight hospitals in Tanzania.

The patient organ doses were estimated using measurements of CT dose indexes (CTDI), exposure-related parameters, and the ImPACT spreadsheet based on NRPB conversion factors. A large variation of mean organ doses among hospitals was observed for similar CT examinations. These variations largely originated from different CT scanning protocols used in different hospitals and scanner type. The mean organ doses in this study for the eye lens (for head), thyroid (for chest), breast (for chest), stomach (for abdomen), and ovary (for pelvis) were 63.9 mGy, 12.3 mGy, 26.1 mGy, 35.6 mGy, and 24.0 mGy,

respectively. These values were mostly comparable to and slightly higher than the values of organ doses reported from the literature for the United Kingdom, Japan, Germany, Norway, and the Netherlands. It was concluded that patient organ doses could be substantially minimized through careful selection of scanning parameters based on clinical indications of study, patient size, and body region being examined. Additional dose reduction to superficial organs would require the use of shielding materials.(Ngaile and Msaki, 2006)

Daryoush Khoramian, Bijan Hashemi. (Khoramian and Hashemi, 2017) presented result of assessed estimate the effective and organ doses in an average human according to 103 and 60 ICRP tissue weighting factor for six common protocols of Multi-Detector CT (MDCT) machine in a comprehensive training general hospital in Tehran/Iran. To calculate the patients' effective dose, the CT-Expo2.2 software was used .Organs/tissues and effective doses were determined for about 20 patients (totally 122 patients) for every one of six typical CT protocols of the head, neck, chest, abdomen-pelvis, pelvis and spine exams .In addition, the CT dosimetry index (CTDI) was measured in the standard 16 and 32 cm phantoms by using a calibrated pencil ionization chamber for the six protocols and by taking the average value of CT scan parameters used in the hospital compared with the CTDI values displayed on the console device of the machine. The values of the effective dose based on the ICRP 103 tissue weighting factor were: 0.6, 2.0, 3.2, 4.2, 2.8, and 3.9 mSv and based on the ICRP 60 tissue weighting factor were: 0.9, 1.4, 3, 7.9,4.8 and 5.1 mSv for the head, neck, chest, abdomen-pelvis, pelvis, spine CT exams respectively .Relative differences between those values were-22, 21, 23,-6,-31 and 16 percent for the head, neck, chest, abdomen-pelvis, pelvis, spine CT exams, respectively. The average value of $CTDI_{vol}$ calculated for each protocol was: 27.32±0.9, 18.08±2.0, 7.36±2.6, 8.84±1.7, 9.13±1.5, 10.42±0.8 mGy for the head, neck, chest, and abdomen –

Pelvis and spine CT exams, respectively.

The highest organ doses delivered by various CT exams were received by brain (15.5 mSv), thyroid (19.00 mSv), lungs (9.3 mSv) and bladder (9.9 mSv), bladder (10.4 mSv), stomach (10.9 mSv) in the head, neck, chest, and the abdomen-pelvis, pelvis, and spine respectively .Except the neck and spine CT exams showing a higher effective dose compared to that reported in Netherlands, other exams indicated lower values compared to those reported by any other country.(Khoramian and Hashemi, 2017)

Adnan Lahham, Hussein ALMasri (Lahham and ALMasri, 2018) presented result of assessed A total of 120 adult female and male patients randomly selected from 10 hospitals in the West Bank and Gaza Strip were investigated for organ and effective doses from abdominal computed tomography scan .The organs considered in this study are liver, stomach and colon .Assessment of radiation doses was performed by using a commercially available Monte Carlo based software Virtual Dose™ CT, a product of Virtual Phantoms, Inc. The software utilizes male and female tissue equivalent mathematical phantoms of all ages and sizes from new born up to morbidly obese patients .The corresponding phantom was selected for every patient according to patient's demographic parameters .Patient demographic data, scanning parameters and dose indicators (including patient body mass index (BMI), milliampere-second (mAs), X-ray tube kilovoltage (kVp), computed tomography dose index ($CTDI_{vol}$), dose length product (DLP),manufacturer, name and type of operated CT scanner) were recorded for every examination. The collected parameters were used to calculate the organ and effective doses for every patient .The highest estimated patient organ doses were 25 mGy for liver, 20 mGy for stomach and 30 mGy for colon for a male patient with BMI of 30 kg/m2and 90 kg of weight. This patient correspondent effective dose was 9 mSv. The average effective dose for the entire patient population was 5.5 mSv with a range between 2 and 10 mSv .The highest effective dose was found for a female patient with a BMI of 26.6 kg/m2, and 77 kg of weight. This patient

correspondent organ doses were 14, 9 and 14 mGy for the liver, stomach and colon, respectively. The average organs doses per patient estimated for patients from all investigated hospitals were 13.1, 7.6 and 13.2 mGy for liver, stomach and colon, respectively .Both effective dose and organ doses increase with BMI and body weight .In general, the estimated radiation doses from abdominal CT examinations.(Lahham and ALMasri, 2018)

M.K.A. KARIM*, S. HASHIM, A. SABARUDIN, D.A. BRADLEY & N.A. BAHRUDDIN: .(Karim et al., 2016) presented result of assessed doses from CT scan procedures and its related risks to the patients from five hospitals in Johor State, Malaysia were analyzed. The survey was conducted in a two-month period encompassing data for 460 patients with the number for each hospital being set at 32, 30 and 30 samples for CT brain, CT thorax and CT abdomen, respectively. The results indicated that the CTDIw, DLP and effective dose values ranged from 7.0±1.3 to 67.7±3.4 mGy, 300.2±135.4 to 1174.2±79.9 mGy.cm and 1.5±0.2 to 11.7±6.65 mSv, respectively. The organ doses were calculated using CT EXPO software (Ver. 2.3.1, Germany) and were found to vary within the hospitals and the type of the CT examinations. Effective cancer risks per procedure were calculated by multiplying organ dose with the nominal cancer risk that was adapted from International Commission on Radiological Protection (ICRP) Publication 103. The values ranged from 0 to 1449 cancer cases per one million procedures for these three routine examinations. This present work showed that the CT systems can impart high radiation doses and increase of radiation risk to patients if optimization protocols are ignored.(Karim et al., 2016)

1S J FOLEY, BSc, PGDip, data were collected for 3305 patients. 30 sites responded with data for 34 scanners, representing 54% of the national total. All equipment had multi slice

Capability (2–128 slices). DRLs are proposed using CTDIvol (mGy) and DLP (mGy cm) for CT head (66/58 and 940, respectively), sinuses (16 and 210, respectively),

cervical spine (19 and 420, respectively), thorax (9/11 and 390, respectively), high resolution CT and 280, respectively, CT pulmonary angiography (13 and 430, respectively), multiphase abdomen (13 and 1120, respectively), routine abdomen/pelvis (12 and 600, respectively) and trunk examinations (10/12 and 850, respectively). These values are lower than current DRLs and comparable to other international studies. Wide variations in mean doses are noted across sites. Conclusions: Baseline for Irish CT DRLs are provided on the most frequently performed CT examinations. The variations in dose between CT departments as well as between identical scanners suggest a large potential for optimization examinations.

Chapter Three

Materials & Method

3.1. Materials:

3.1.1. Machines:

The CT scanners used in this study were (CT General Electric 16 slice)

3.1.2 Population:

In this study the data of CT-scanner has been collected from three hospitals (A - B - C), in Khartoum in 2019. which consist on survey for scanner parameters and equipment's. Data were used to assess doses for 60 adult patients' abdomen-pelvis CT examinations. The local ethics committees of all participating institutions approved the study protocol. The collected information in regard to:

o Made/model/year of installation,

- CT equipment-specific information

o Made/model/year of installation,

o Number of slices

All hospital in this study hospitals (A - B - C) use GE Model light speed 16 slices, all equipment installed 2019

- Patient demographic data

o Age of patient in this study between (18 - 85) years for hospital A ,(25 - 75) years for hospital B and (18 - 95) years for hospital C ,the number of male for hospital A is 11and female 9 ,the number of male for hospital B is 15 and female 5 ,the number of male for hospital C is 6 and female 14 the number of examination covered in this study 60

Table 3.1 patient population of the study classified per hospital and type of examination.

Hospital	Female	Male	Total
Hospital A	9	11	20
Hospital B	5	15	20
Hospital C	14	6	20
Total	28	32	60

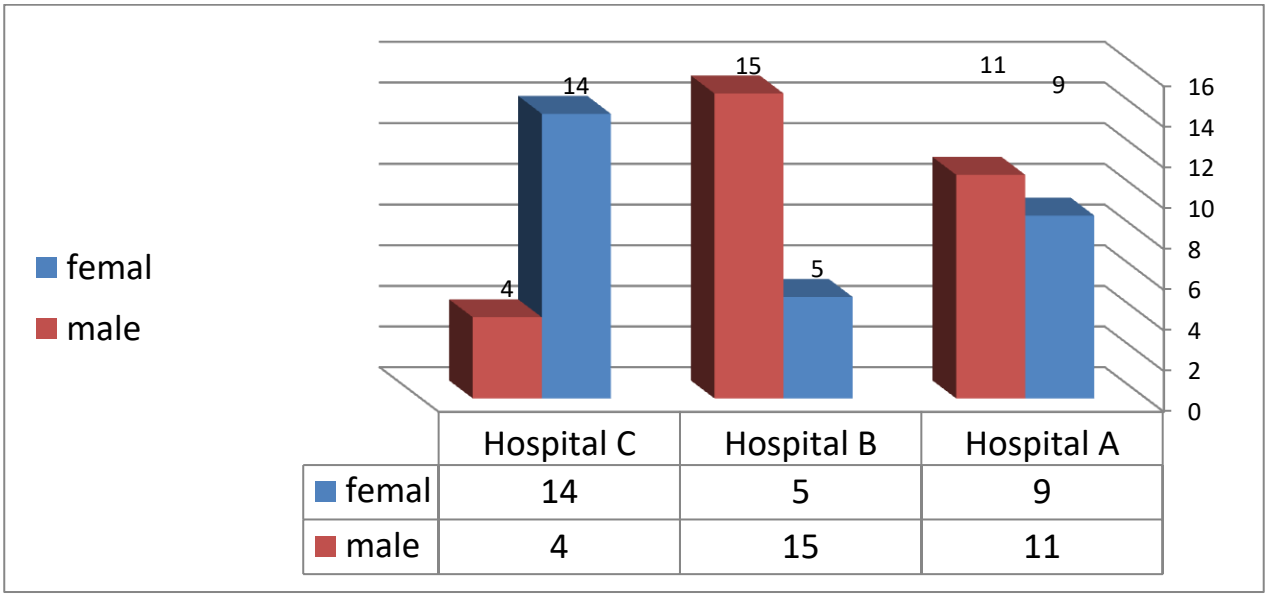

Figure 3.1: Compare the female and male in three hospitals

3.2. Methods:

3.2.1 Data Collection:

The data were collected using a sheet for all patients in order to maintain consistency of the information from display.

A data collected sheet was designed to evaluate the patient doses, the collected data included demographic information (sex and age), scan parameters (KV, mAs, slice thickness, scan time, number of slice, and scan length), and dosimetric information (CTDI, and DLP).

3.2.2. Dosimetric calculations:

CT Expo software will used to calculate common CT dose descriptors: (i) CT weighted dose index ($CTDI_W$) and volume dose index ($CTDI_{vol}$) provides an indication of the average absorbed dose in the scanned region, (ii) CT dose – length product (DLP) the integrated absorbed dose along a line parallel to the axis of rotation for the complete CT examination, and (iii) effective dose (E): a method for comparing patient doses from different diagnostic procedures (Effective dose)

3.2.3. CT-Expo V 2.5 software:

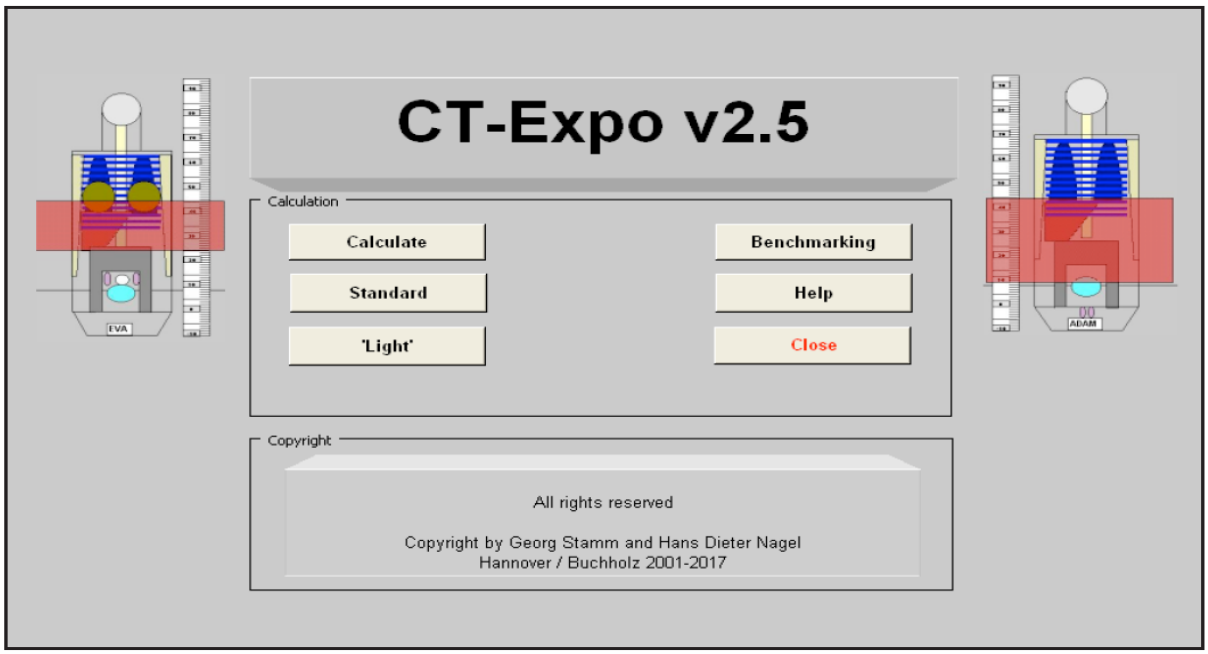

Figure 3.2: CT –Expo v2.5

In this study was used CT-Expo Version 2.5 software tool for dose calculations and CT-Expo tools—based on Monte Carlo data published by the Research Center for Environment and Health in Germany—for dose calculation. Dose estimation is done based on mathematical phantoms for adult (ADAM and EVA)

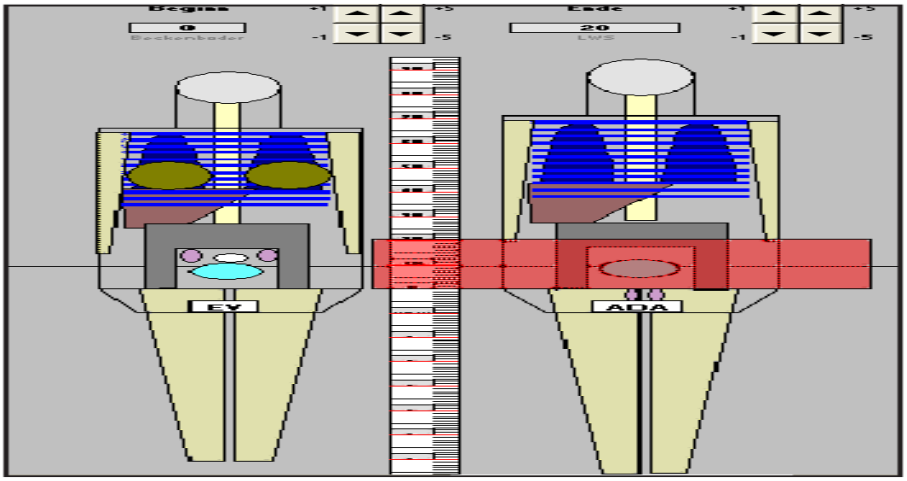

Figure 3.3: mathematical phantom (ADAM, EVA)

The software allows the calculations of the CT dose descriptors ($CTDI_{vol}$ and DLP), organ doses and effective dose in accordance with new recommendations of the international commission for radiological protection ICRP 103[15].

CT scan parameters

- kV, mA, rotation time and scan time (spiral mode),
- Scan length (start and end of scan region),
- Number of slices, slice thickness, pitch.

3.3. In put steps:

In this section, the procedure to enter the data required for dose calculations is described step-by-step

- **Selection of Patient Type**

The type of patient for which dose calculation shall be made is defined by selecting the age group (adult, children, and babies) and the sex (male, female).

- **Selection of Scan Range**

The scan range can directly be defined by entering numerical values of the lower and the upper limits of the scan area

- **Selection of Scanner Model**

The scanner model for which dose calculation shall be performed by selecting the scanner manufacture and the type of scanner

- **Input of Scan Parameters**

The input of actual scan parameters is made in the cells kept in white (fig. 3.4). The following set of parameters is required:

Tube voltage U [KV] -

Tube current I [mA]-

Acquisition time t [s] -

Alternatively: current-time product Q [mAs]-

Total collimation N.hcol [mm]-

Table feed TF [mm]-

Reconstructed slice thickness hrec [mm] Number of scan series [ser.]

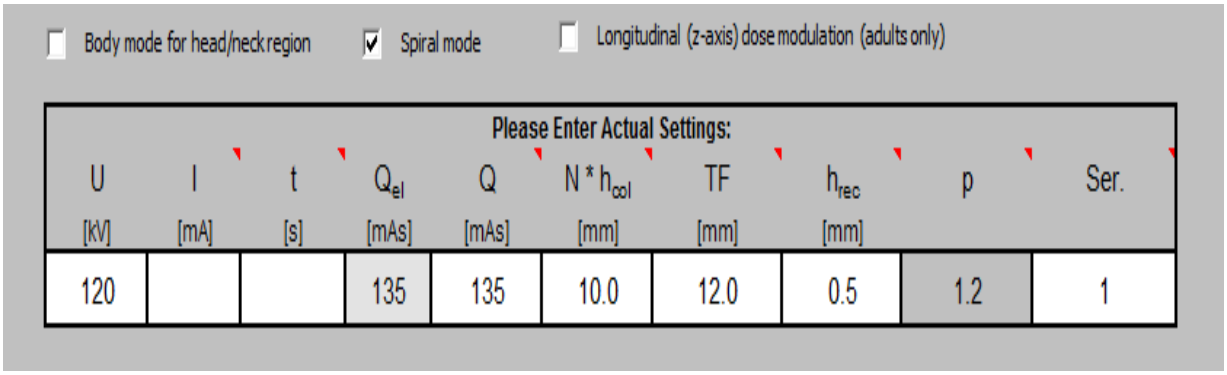

Fig 3.4: Scan parameter

- **Results**

Results for the following dose quantities are displayed in the yellow shaded cells (fig. 3.5):

CTDIW [mGy]: Weighted CTDI per scan (=slice or rotation)

CTDIvol [mGy]: volume CTDI (also; effective CTDI (CTDIW, eff)) per scan

DLPW [mGy.cm]: Dose-Length Product (based on CTDIW) per scan series

E [mSv]: Effective dose per scan series

Dusters [mSv]: Uterine dose per scan series

HT [mSv]: Organ dose per scan series

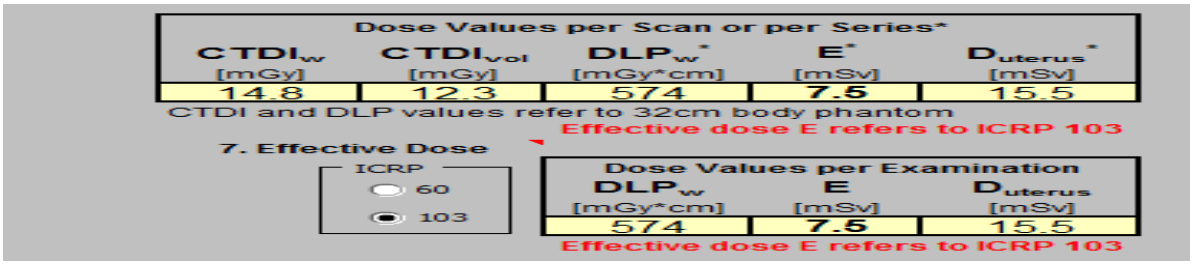

Figure (3.5): Results

- **Calculation mode for effective dose**

The calculation of effective dose can be performed either according to the previous method

(ICRP 60) or the new method (ICRP 103)

Tissue or Organ	H_T per Series [mSv]	Tissue or Organ	H_T per Series [mSv]
Brain	0.0	Upp. large int.	16.9
Salivary glands	0.0	Thymus	0.1
Thyroid	0.0	Spleen	7.9
Breasts	0.3	Pancreas	5.3
Oesophagus	0.1	Adrenals	2.5
Lungs	0.5	Kidneys	15.0
Liver	7.9	Small intest.	16.3
Stomach	10.3	Uterus	15.5
Low. Large int.	16.1	Prostate	0.0
Testicles	0.0	Gall bladder	5.3
Ovaries	15.9	Heart	0.5
Bladder	17.9	ET tissue	0.0
Bone marrow	7.3	Oral mucosa	0.0
Bone surfaces	12.0	Lymph nodes	9.3
Skin	7.4	Muscle	9.3
		Eye lenses	0.0

Figure (3.6): Organ dose

3.5. Data Analysis

The data in this study were analysis by using Microsoft Excel and SPSS software**.**

Chapter Four

Results and Discussion

4.1. Results:

The results are presented for dose measurements performed in three CT units and 60 patients. Doses were estimated in terms of CTDIvol, DLP and E

Table (4.1): summaries the characteristic performance parameters for the CT systems and console displayed form The CT scanner G E model Acquilion (16-slice) hospital **A**

	mean	median	Standard deviation	maximum	minimum
Age	47	46	19.2	95	18
KV	120	120	0	120	120
mAs	114.8	120	37	240	60
San length	43.2	43.4	34.9	50.5	37
Pitch	1.2	1.2	0	1.2	1.2
CTD_{VOL}	10.2	10.2	3.5	22.1	5.3
DLP	497.9	501.6	205	1184	225

Table (4.2): summaries the characteristic performance parameters for the CT systems and console displayed form The CT scanner G E model Acquilion (16-slice) hospital **B**

	mean	median	Standard deviation	maximum	minimum
Age	49	50	21	85	18
KV	120	120	0	120	120
120mAs	147.8	142.1	42.8	270	70
San length	44.61	44.68	1.69	47.27	41.64
Pitch	1.2	1.2	0	1.2	1.2
CTD_{VOL}	8.45	7.69	2.68	13.49	5.03
DLP	410.25	366.78	128.63	720.22	267.34

Table (4.3) summaries the characteristic performance parameters for the CT systems and console displayed form The CT scanner G E model Acquilion (16-slice) hospital **C**

	mean	median	Standard deviation	maximum	minimum
Age	49.3	46.5	21.2	85	18
KV	120	120	0	120	120
mAs	81.5	75	29.3	143	50
San length	48.9	49	0.16	51.5	44.5
Pitch	1.2	1.2	0	1.2	1.2
CTD_{VOL}	7.4	7.1	2.62	11.9	3
DLP	385.5	365.1	140.3	622.4	156.9

Table (4.4) show the estimation of mean $CTDI_W$, $CTDI_{vol}$, DLP and effective dose calculated by CT-Expo Version 2.5 software were used data collection form CT scanner G E model Acquilion (16-slice) hospital **A**

	mean	median	Standard deviation	maximum	minimum
$CTDI_w$	11.9	13.2	2.7	14.8	6.6
$CTDI_{vol}$	9.9	11	2.2	12.3	5.5
DLP	450.7	502.4	120.5	604.2	230.2
E	7.6	7.5	2.5	12.2	3.9

Table (4.5) show the estimation of mean$CTDI_W$, $CTDI_{vol}$, DLP and effective dose calculated by CT-Expo Version 2.5 software were used data collection CT scanner G E model Acquilion (16-slice) hospital **B**

	mean	median	Standard deviation	maximum	minimum
$CTDI_w$	10.56	9.79	3.13	16.64	6.85
$CTDI_{vol}$	8.80	8.15	2.61	13.87	5.71
DLP	410.95	362.38	122.63	671.54	266.79
E	5.39	4.71	1.89	9.64	3.08

Table 4.6 show the estimation of mean$CTDI_W$, $CTDI_{vol}$, DLP and effective dose calculated by CT-Expo Version 2.5 software were used data collection CT scanner G E model Acquilion (16-slice) hospital **C**

	mean	median	Standard deviation	maximum	minimum
$CTDI_w$	10.3	9.9	3.5	16.5	4.4
$CTDI_{vol}$	7.5	7.2	2.5	12	3.2
DLP	380.4	356	131.50	605.3	161.40
E	6.30	5.62	2.4	10.6	2.42

Table

4.7 show that the average equivalent dose per mSv for some organs during abdomen CT examination

Organ-mSv / Hospital	Stomach	Spleen	Pancreas	Adrenals
A	13.67	13.06	10.52	9.03
B	11.64	11.55	9.45	9.22
C	11.39	11.36	9.42	9.21

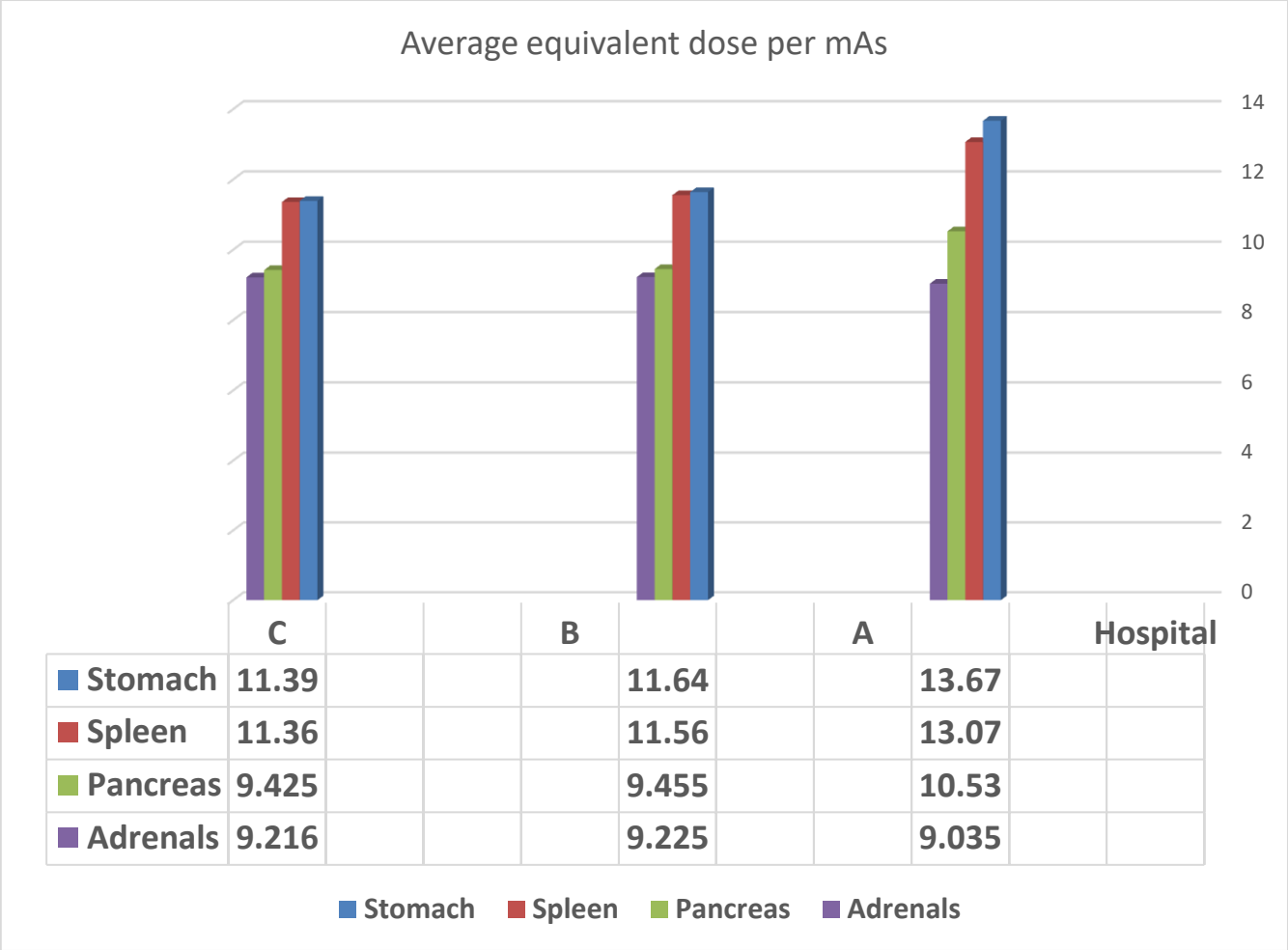

Figure 4.1. Show that the average equivalent dose per mSv for some organs during abdomen Ct examination

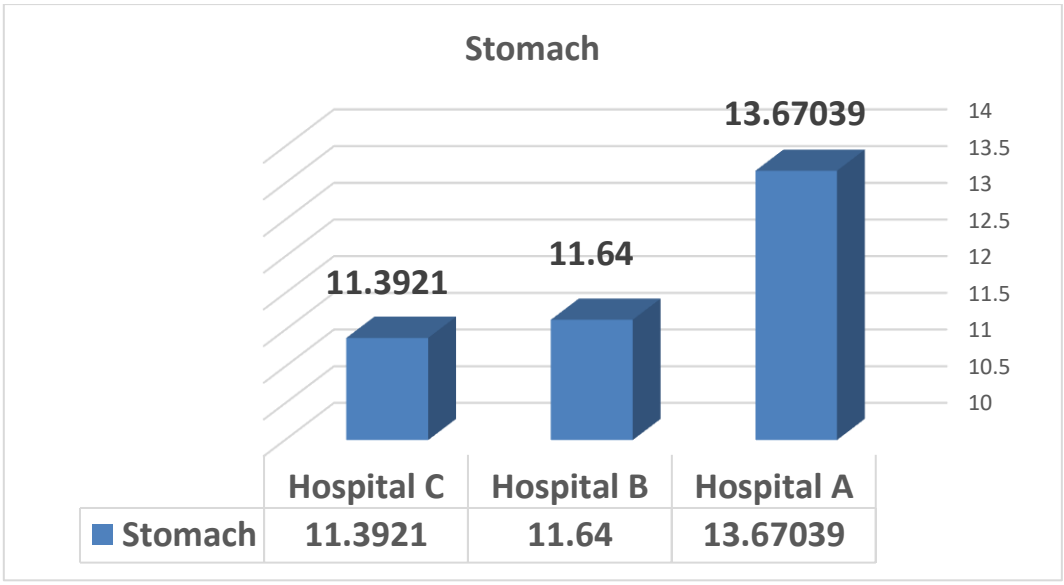

Figure 4.2. Compare the equivalent dose per mSv for stomach between three hospitals (A-B-C) during CT examination

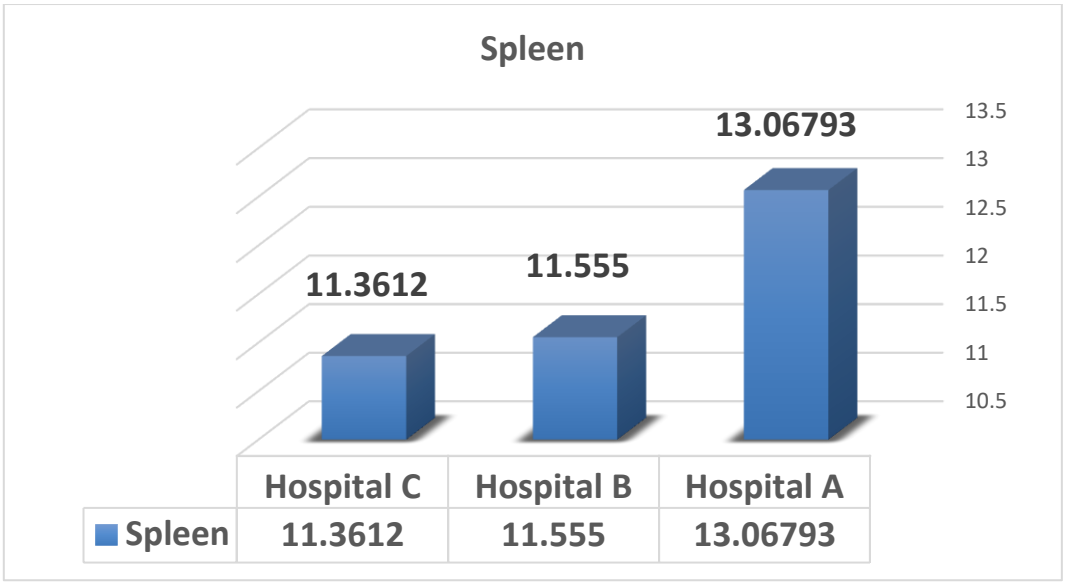

Figure 4.3. Compare the equivalent dose per mSv for spleen between three hospitals (A-B-C) during CT examination

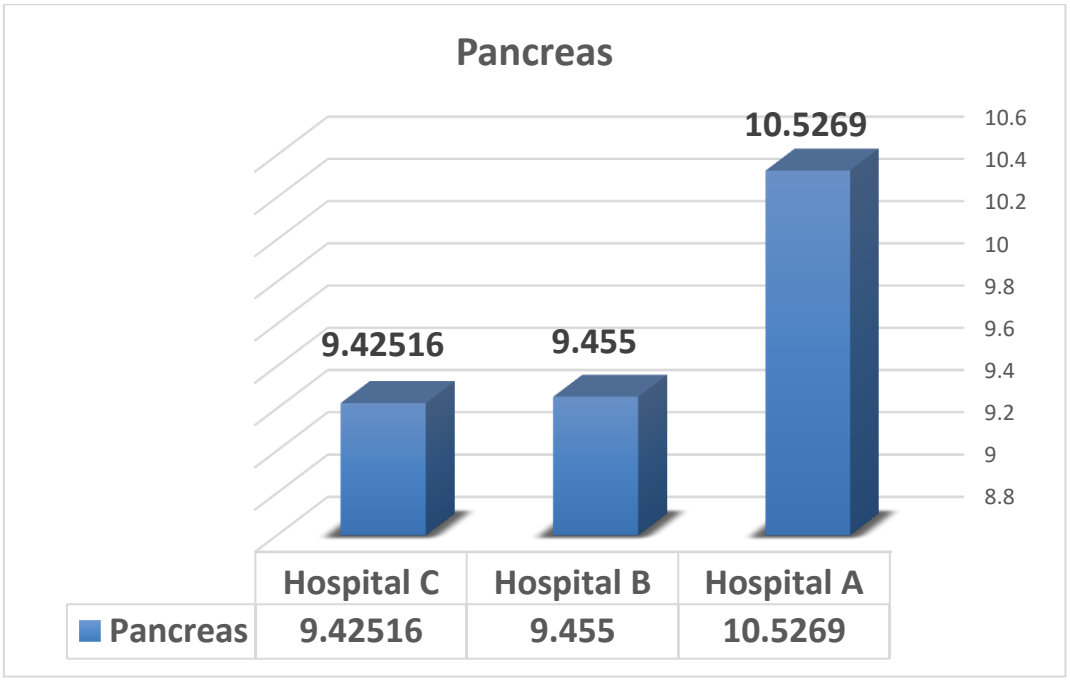

Figure 4.4. Compare the equivalent dose per mSv for pancreas between three hospitals (A-B-C) during CT examination

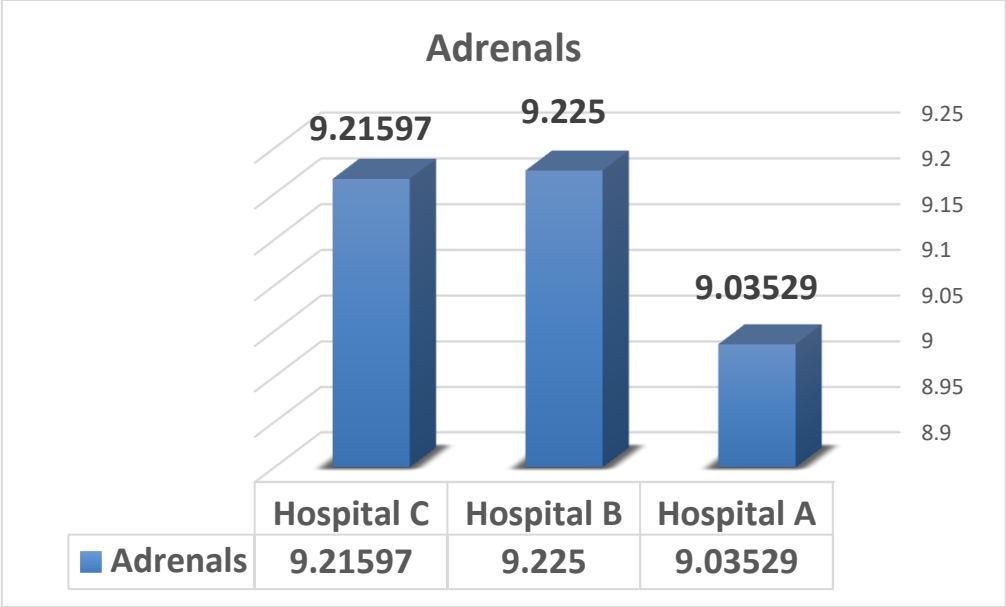

Figure 4.5. Compare the equivalent dose per mSv for adrenals between three hospitals (A-B-C) during CT examination

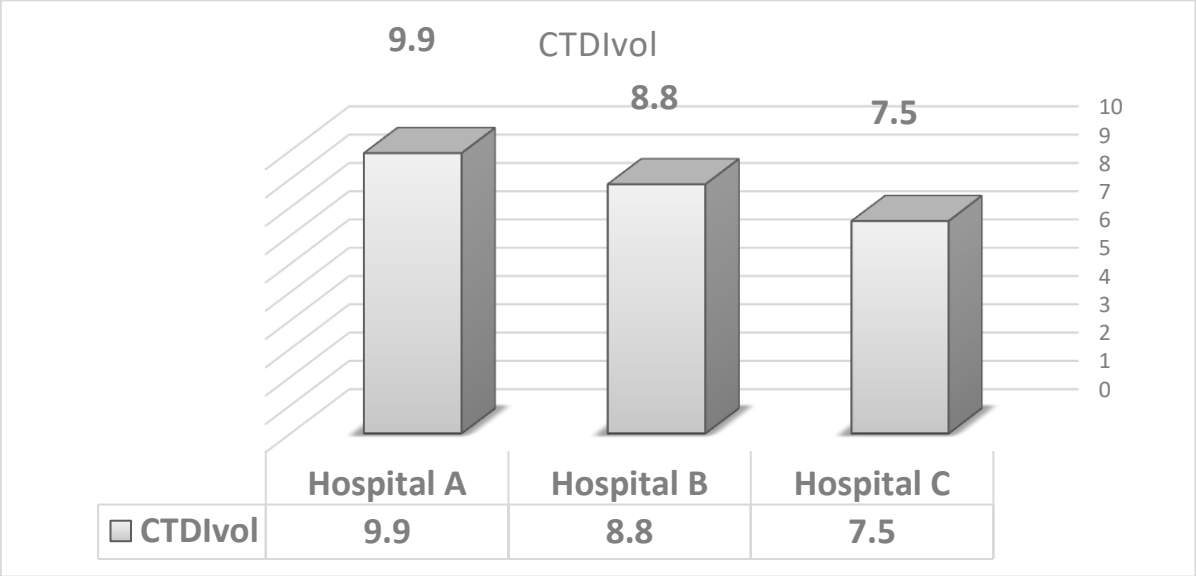

Figure (4.6) compare the $CTDI_{vol}$ between three hospitals (A-B-C)

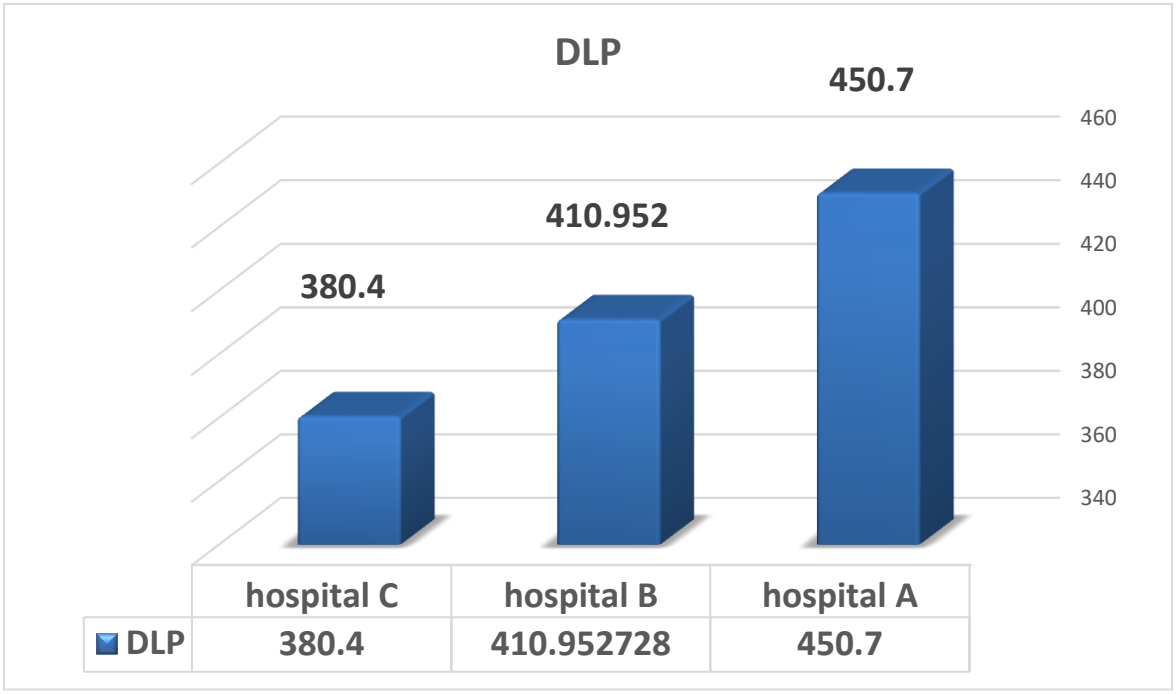

Figure (4.7) compare the DLP between three hospitals (A-B-C)

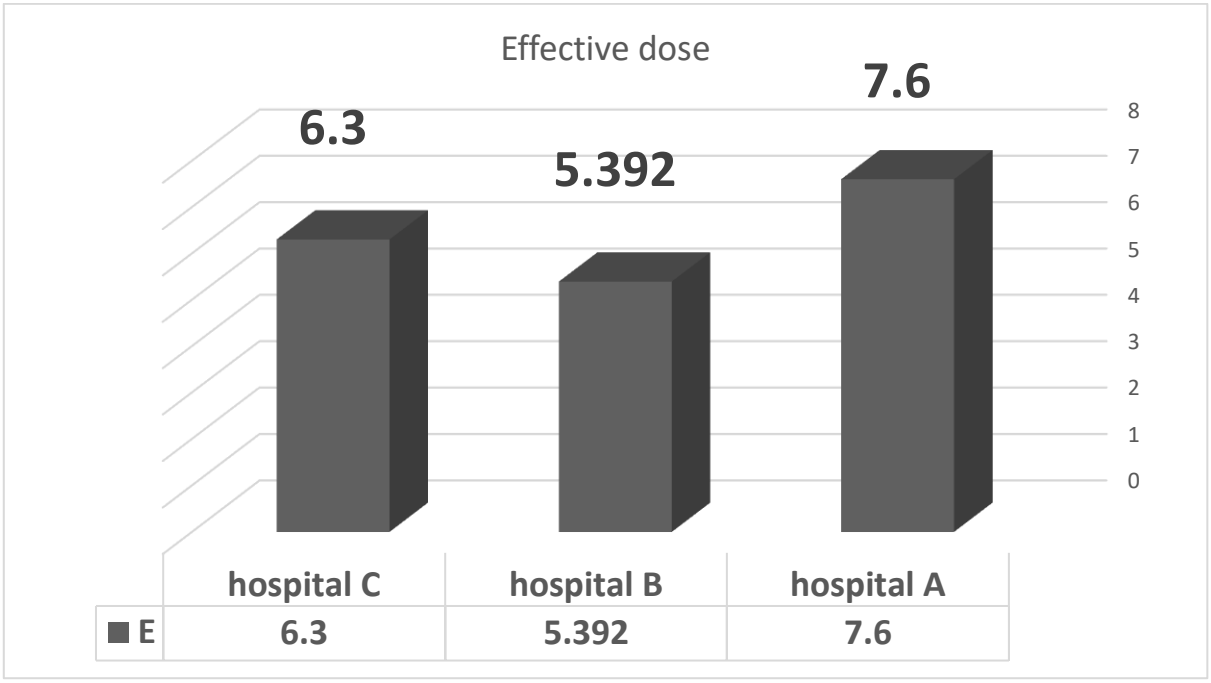

Figure (4.8) compare the effective dose (E) between three hospitals (A-B-C)

Table (4.8) show the mean of CTDI, DLP and E in this study and compare with other country and EC reference dose:

country	This study	Malaysia	EC	Switzerland	Ireland	Iran
$CTDI_{vol}$	8.73	10.22	16.95	15	12	9.1
DLP	414.01	450	780	650	600	410.8
E	6.43	6.75	11.7	9.3	9	6.162

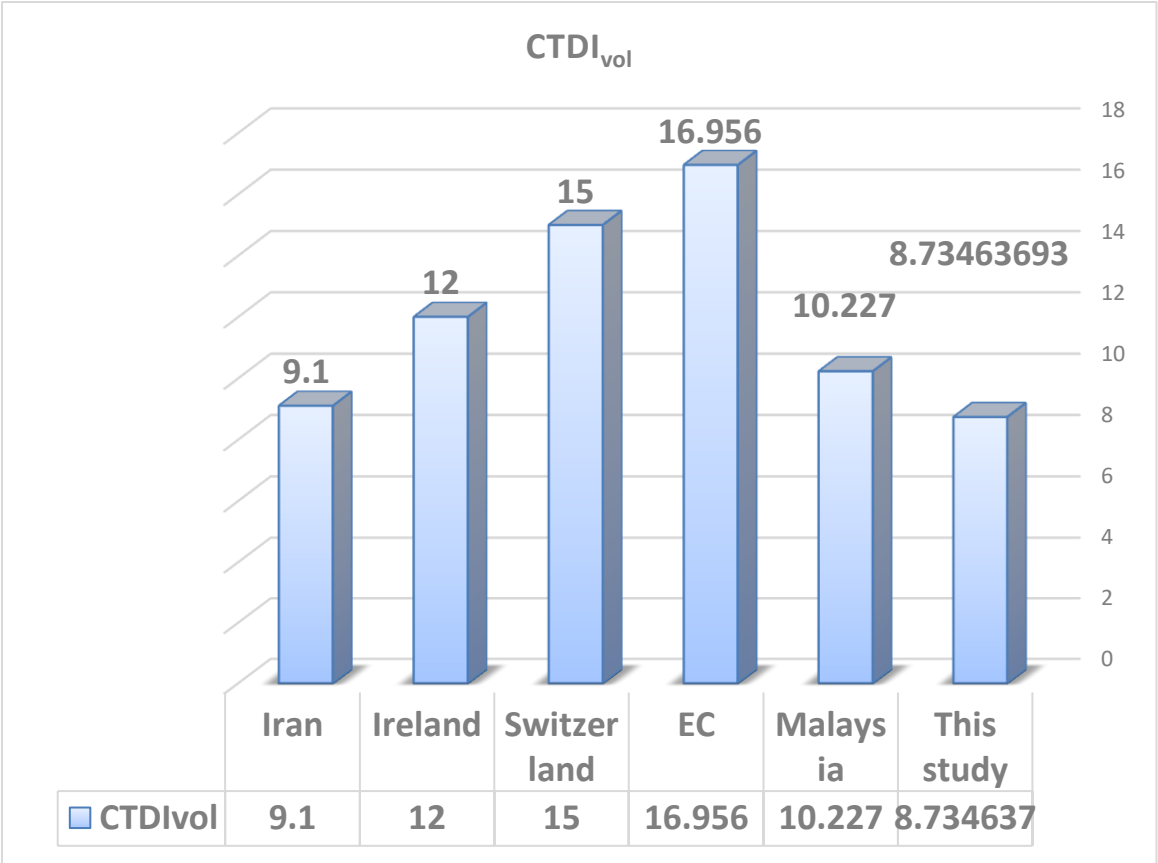

Figure (4.9) show that the dose presented ($CTDI_{vol}$)

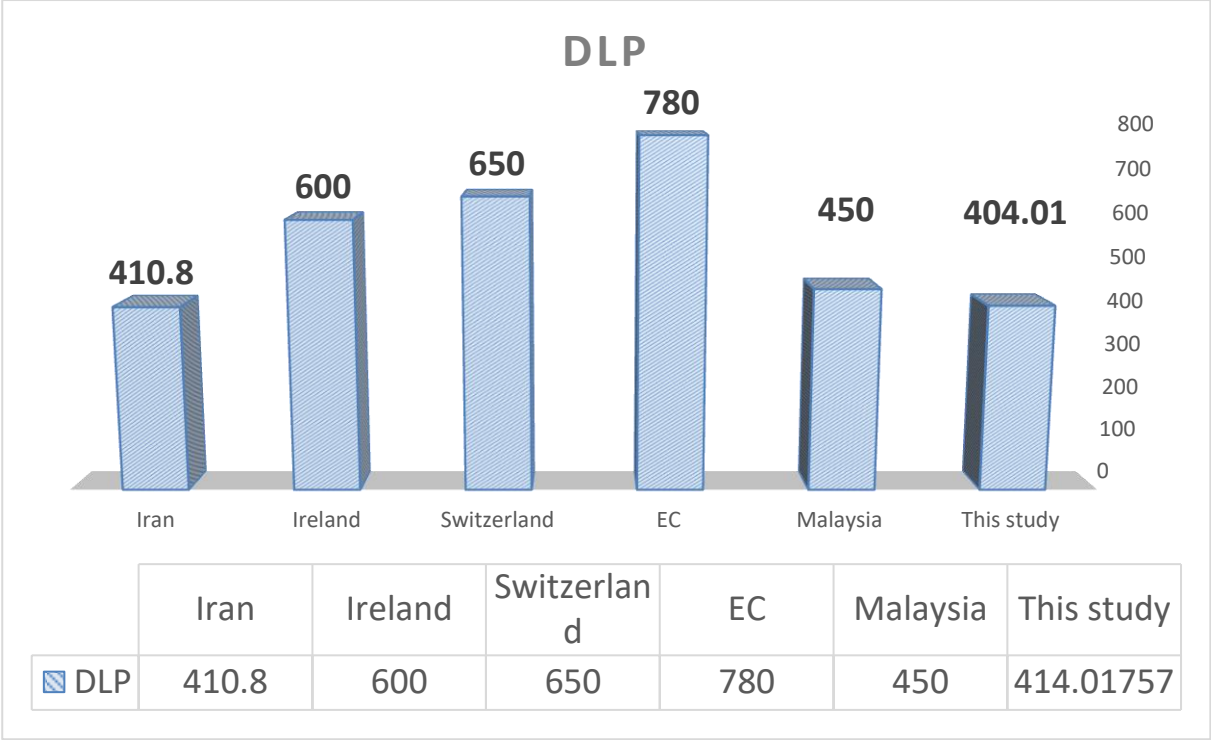

	Iran	Ireland	Switzerland	EC	Malaysia	This study
DLP	410.8	600	650	780	450	414.01757

Figure (4.10) show that the dose presented (DPL)

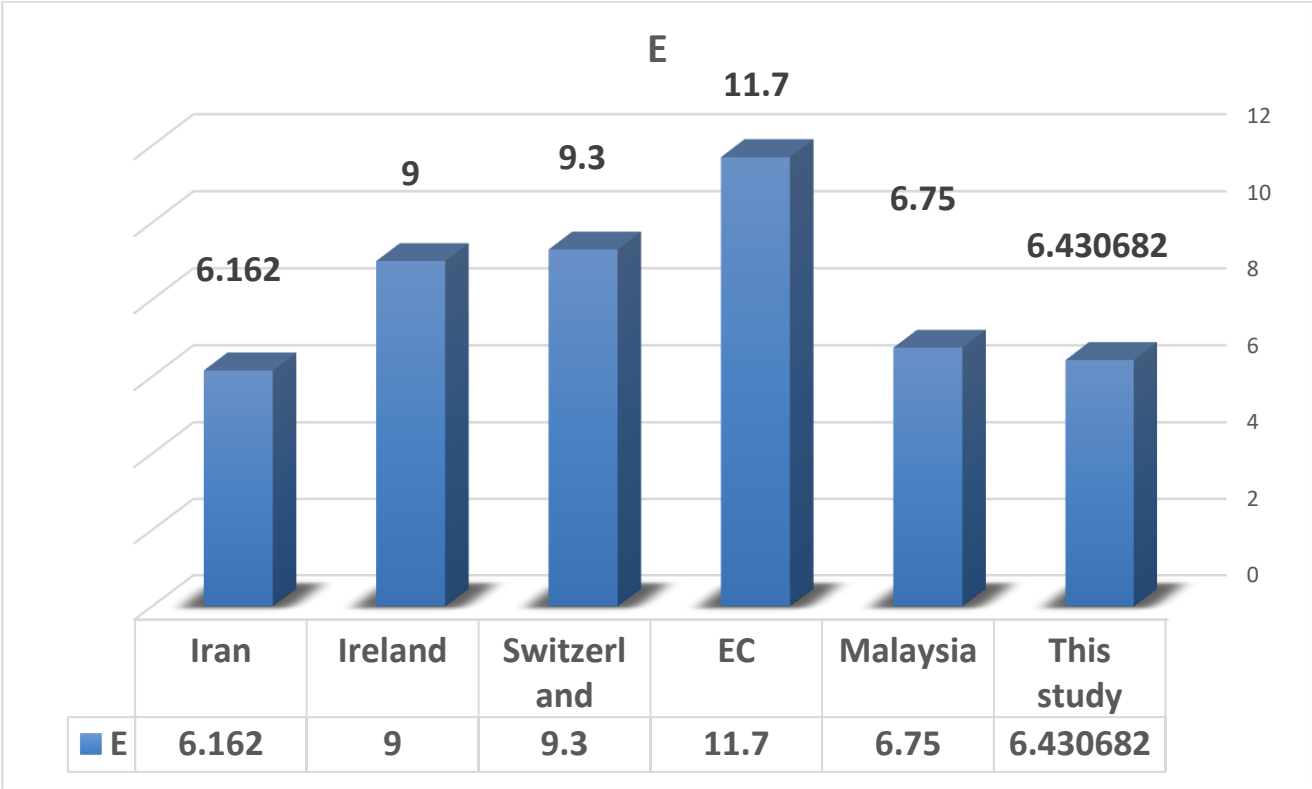

	Iran	Ireland	Switzerland	EC	Malaysia	This study
E	6.162	9	9.3	11.7	6.75	6.430682

Figure (4.11) show that the dose presented (E

Chapter Five

Discussion, Conclusion and Recommendations

5.1. Discussion:

In this study doses were expressed in terms of CTDIvol, DLP, and E. This provide an indication of the average absorbed dose in the scanned region ($CTDI_{vol}$), the integrated absorbed dose along a line parallel to the axis of rotation for the complete CT examination (DLP), and comparing the effective dose between three hospitals, below we will discussion of the result in detail.

Table **(**4.1) and (4.5) from result represented the estimation of (mean, median, STD, min and max) and CTDI, DLP, E, PITCH calculated by software CT expo 2.5, were used data collection from CT scanner GE General Electric model light speed 16 slice three hospitals (A), (B) and (C) are used same protocol(automatic) and show the three hospitals have different mean $CTDI_{vol}$ (9.9 mGy), (8.8 mGy) and (7.3 mGy) respectively the different mean DLP (450 mGy*cm), (410 mGy*cm) and (380 mGy*cm) respectively and different mean Effective dose (E) (7.6 mSv), (5.3 mSv) and (6.3 mSv) respectively although used the same protocol the doses are different because the automatic exposure is change depend on the area irradiated(tissue density) and some parameter such as the slice thickness which affects the pitch which affects to the doses.

Table (4.7) from result represented the patient equivalent organ doses (stomach, spleen, pancreas and adrenals) were estimated calculated by software CT expo 2.5, were used data collection from CT scanner GE General Electric model light speed 16 slice three hospitals (A), (B) and (C) using measurements of CT dose indexes (CTDI), exposure-related parameters, and the ImPACT spreadsheet based on National Radiological Protection Board (NRPB) conversion factors. Alight variation of mean organ doses among hospitals (A-B-C) was observed for similar CT examinations. These variations largely originated from different CT scanning protocols used in different hospitals (A-B-C).

Figure (4.8) compare the effective dose (E) between three hospitals (A-B-C) In figure 4.6 to 4.8 show that the hospital B has higher dose than hospital C and Abut hospital C has less dose for all hospitals. In table 4.8 and figure 4.9 to 4.10 show that the dose presented (CTDI $_{vol}$, DLP and E) in this study is less than similar study in some country such as EC, Malaysia Switzerland and Ireland but higher than Iran. In table (4.8) showed that some organ dose during abdomen CT scan the stomach has higher dose (12.23 mSv) than the spleen (11.99 mSv) and spleen has higher dose than pancreas (9.8 mSv) and adrenal has less one dose (9.158 mAs).

5.2. Conclusion:

The aims of this study are determine the effective dose and some organs dose of the patients undergoing abdomen CT examination by three hospitals. The effective dose was (6.43068 mSv) and dose from the organs Stomach, Spleen, Pancreas and Adrenals (12.23, 11.99, 9.8 and 9.158) mSv respectively.

- The effective dose in this study was compared them with different reported values from the Malaysia, EC, Switzerland, Ireland and Iran so the effective dose resulted as (This study for 6.43mAs, Malaysia 6.75mAs, EC 11.7mAs, Switzerland 9.3mAs, Ireland 9mAs, Iran 9 mAs)
- The effective dose in this study was compared them with different reported values from the Malaysia, EC, Switzerland, Ireland and Iran reference and it was the lowest effective dose. This difference in effective and organ doses refer to the difference in protocols.
- The effective dose in this study was compared them with different reported values (This study for 6.43mAs, Malaysia 6.75mAs, EC 11.7mAs, Switzerland 9.3mAs, Ireland 9mAs, Iran 9 mAs)
- To compared the effective dose between the three hospitals (A – B and C), hospital A 7.6 mAs, hospital B 5.3 mAs and hospital C 6.3 mAs

5.3. Recommendations:

- Must evaluation of using automatic mAs to achieve the optimization.
- Must reducing the scan range of the abdomen so as to avoid the unnecessary dose from exposure and thus reducing effective dose.
- recommend the results of this study are taken into consideration to establish the DRLs to Sudan.
- Optimization of protection should be conducted to the radiological departments by establishing standard protocol in the Sudan and commitment to quality control program.

Reference:

AHMAD, S. A. M. 2017. *Classification of Normal Brain Tissues in Computed Tomography Radiographs Using Image Texture Analysis.* Sudan University of Science and Technology.

ALI, M. 2005. Trends in CT abdominal doses in Malaysian practices.

ASSOCIATION, O. H. .2006 Computed tomography radiation safety issues in Ontario.

BOONE, J. M. 2012. CT dose estimation.

BUSHBERG, J., SEIBERT, J., LEIDHOLDT JR, E. & BOONE, J. 2003. The essential physics of medical imaging. 2002. *Eur J Nucl Med Mol Imaging,* 30**,** 1713.

DANCE ,D., CHRISTOFIDES, S., MAIDMENT, A., MCLEAN, I. & NG, K. 2014a. Diagnostic radiology physics. *International Atomic Energy Agency*.

DANCE, D., CHRISTOFIDES, S., MAIDMENT, A., MCLEAN, I. & NG, K. 2014b. Diagnostic radiology physics: A handbook for teachers and students. Endorsed by: American Association of Physicists in Medicine, Asia-Oceania Federation of Organizations for Medical Physics, European Federation of Organisations for Medical Physics.

HASSAN, O. A. M. 2012. *Estimation of Patient's Effective Dose during Routine Computed Tomography Examinations.* sudan university of science and technology.

HUDA, W., MAGILL, D. & HE, W. 2011. CT effective dose per dose length product using ICRP 103 weighting factors. *Medical physics,* 38**,** 1261-1265.

KARIM, M., HASHIM, S., SABARUDIN, A., BRADLEY, D. & BAHRUDDIN, N. 2016. Evaluating organ dose and radiation risk of routine CT examinations in Johor Malaysia. *Sains Malaysiana,* 45**,** 567-73.

KHORAMIAN, D. & HASHEMI, B. 2017. Effective and organ doses from common CT examinations in one general hospital in Tehran, Iran. *Polish Journal of Medical Physics and Engineering,* 23**,** 73-79.

LAHHAM, A. & ALMASRI, H. 2018. estimation Of Radiation Doses From Abdominal Computed Tomography Scans. *Radiation protection dosimetry*, 182**,** 235-24.0

NGAILE, J. E. & MSAKI, P. K. 2006. Estimation of patient organ doses from CT examinations in Tanzania. *Journal of applied clinical medical physics,* 7**,** 80-94.

PRINS, R. D., THORNTON, R. H., SCHMIDTLEIN, C. R., QUINN, B., CHING, H. & DAUER, L. T. 2011. Estimating radiation effective doses from whole body computed tomography scans based on US soldier patient height and weight. *BMC medical imaging,* 11**,** 20.

SADRI, L., KHOSRAVI, H. & SETAYESHI, S. 2013. Assessment and evaluation of patient doses in adult common CT examinations towards establishing national diagnostic reference levels. *Int. J. Radiat. Res,* 11**,** 245-252.

VALENTIN, J. 2007. *The 2007 recommendations of the international commission on radiological protection*, Elsevier Oxford.

1S J FOLEY, BSc, PGDip, 2M F MCENTEE, BSc, PhD and 1L A RAINFORD, BSc, PhD

1School of Medicine and Medical Science, University College Dublin, Dublin, Ireland, and 2Discipline of Medical Radiation Sciences, Faculty of Health Science, University of Sydney, Australia

5.4 Appendix

Patient info.			Scan parameters											Console displayed dose	
NO	Sex M/F	Age	kV	(mA)	mAs	Slice thickness (mm)	pitch	Speed	Total scan time (s)	Number of slice	Table movement		Scan length (cm)	CTDIvol	DLP
											Start	End			
1															
2															
3															
4															
5															
6															
7															
8															
9															
10															
11															
12															
13															
14															